MARANGONI INSTABILITIES UNDER MICROGRAVITY AND IN LIQUID–LIQUID SYSTEMS WITH AN INTERFACIAL CHEMICAL REACTION

Thesis submitted for the degrees of

Doctor of Philosophy

and

Diploma of Imperial College

in the Faculty of Engineering of the

University of London

by

MARIA ALCINA DE OLIVEIRA CRUZ MENDES TATSIS

M.Phil.

Department of Chemical Engineering and

Chemical Technology,

Imperial College of Science, Technology and Medicine,

London SW7

February 1990

ABSTRACT

In this work the onset of Marangoni instabilities in liquid–liquid systems with a reversible pseudo first–order chemical reaction taking place at the interface is investigated. This type of system is a simplified model of extractive processes of industrial interest in which Marangoni instabilities have been observed.

Since in some systems the heat of reaction may be substantial, thermally induced Marangoni flows were considered in addition to Marangoni perturbations produced by local changes of interfacial tension.

In order to decouple possible gravitational instabilities due to the heat of reaction and thermal Marangoni instabilities, experiments were conducted in non–reactive systems under the microgravity conditions achieved in the NASA KC–135 parabolic flights. Results indicated that thermal effects were strong enough to induce Marangoni instabilities.

Stability criteria for the reactive system were derived by performing a linearised stability analysis of the reactive system. Although heat effects were at first included in the model the complexity of the resulting equations made the stability analysis intractable.

Neglecting heat effects, a numerical analysis of the model covering a wide range of conditions indicates that stationary instabilities can occur when the net flux is in the direction of the phase of higher diffusivity. The inter–relation between molecular diffusivity and rate constant of chemical reaction affects the minimum perturbation required to destabilize the system. In all cases the presence of the interfacial chemical reaction made the system more unstable than in the case of pure diffusional mass transfer.

To Joanna and George

ACKNOWLEDGEMENTS

I would like to thank Dr. E.S. Ortiz for her kind help, advice and constant support during the course of this work.

I would also like to express my gratitude to Messrs R. King, K. Gurney and R. Wallington for their advice on the design and construction of the cells for the microgravity work, and Dr. F. Carleton and Mr. L. Moulder for their help with the photography.

My sincere thanks to Professor W. Wakeham for providing time and support during the last year of this research.

I would like to acknowledge the European Space Agency for the opportunity to perform experiments under microgravity, and the Science and Engineering Research Council for the award of a grant to finance travelling and subsistence while carrying out the same experiments.

My gratitude to Jeremy for the editing and to Nick for letting me have his printer for such long time.

I am also grateful to Carla, Ian, Lester and all my other friends who always gave moral support while I carried out this work.

LIST OF CONTENTS

LIST OF FIGURES

CHAPTER 1

INTRODUCTION

The need for the understanding of spontaneous interfacial phenomena has been identified in several fields, such as: liquid–liquid extraction, crystal growth from melts, separation of immiscible alloys, formation of fibres and membranes and human biology.

Mass transfer across a liquid–liquid interface has been described in terms of several theoretical models which assume simplified and idealised conditions. For instance, in the design of contact equipment the incomplete knowledge of the physicochemical and hydrodynamic effects at the phase boundary has not permitted the development of correlations which would allow a more accurate estimation of mass transfer coefficients. The problem is further complicated by the presence in some systems of spontaneous interfacial turbulence which produces greater mass transfer coefficients than those predicted by theoretical methods.

Spontaneous interfacial turbulence may be due to the formation of local interfacial tension gradients (Marangoni instabilities), the presence of unstable density gradients (gravitational instabilities) or the interaction of both these effects. While interfacial tension gradients may be created by changes in interfacial concentrations, temperature or electrostatic charges, density gradients may be due to variations in temperature or volume contraction on mixing.

Marangoni convection has been studied for a wide variety of systems and stability criteria to predict the onset of instabilities have already been established for ternary and binary systems. However, although the stability criteria for these two types of systems have been generally confirmed experimentally, there have been disagreements which have

indicated that other destabilising mechanisms may be present. There is experimental evidence that density gradients formed during the transfer of a solute across a liquid–liquid interface play an important role in initiating and promoting interfacial convection generated by interfacial tension gradients. In addition heat effects due to heats of solution or heats of reaction in systems with interfacial chemical reactions, may play an important role in initiating interfacial turbulence. It is therefore important to investigate the relevance of heat and gravitational effects on the mechanism of interfacial turbulence so that they can be included in the mathematical models developed to establish stability criteria.

The purpose of this work was to develop a theoretical model to predict instabilities in liquid–liquid systems when a reversible pseudo first–order chemical reaction occurs at the interface with the release of heat.

This work is divided into two main parts:

(i) Study of the interaction between Marangoni and gravitational instabilities.

(ii) Mathematical modelling and stability analysis of a system with an interfacial chemical reaction.

Part (i) was investigated by performing experiments in a gravitational environment and under the microgravity conditions achieved in the NASA KC–135 parabolic flights. Restrictions on the use of certain chemicals in the parabolic flights led to the use of binary systems at this stage of the work. In Chapter 3 results of these experiments are analysed and interpreted.

In Part (ii) a linearised stability analysis for the reactive system is performed and stability criteria are derived, when heat effects are neglected,

as described in Chapter 4.

A numerical analysis of the interfacial reaction model for a wide range of conditions is reported in Chapter 5.

CHAPTER 2

LITERATURE SURVEY

The literature survey presented here is divided into three main sections: Marangoni instabilities, gravitational instabilities and combined Marangoni and gravitational instabilities. Under each heading only research on liquid–liquid systems and relevant to the work in this thesis is included.

2.1 Marangoni instabilities

2.1.1 Systems with diffusional transfer

Marangoni instabilities are spontaneous interfacial phenomena caused by interfacial tension gradients at the phase boundary. These gradients arise from concentration, temperature or electric potential variations at the interface.

The first to describe and interpret the phenomena was Thomson (1) but it was Marangoni (2) who claimed its discovery.

It was much later that Sternling and Scriven (3) studied mathematically the mechanism of interfacial turbulence in systems where a solute is transferred between two immiscible phases and proposed stability criteria for the prediction of the onset of Marangoni instabilities.

Sternling and Scriven's analysis showed that the stability of these systems depend on the direction of solute transfer and that Marangoni instabilities

" are usually promoted by:

(1) solute transfer out of the phase of higher viscosity,

(2) solute transfer out of the phase in which its diffusivity is lower,

(3) large differences in kinematic viscosity and solute diffusivity between the two phases,

(4) steep concentration gradients near the interface,

(5) interfacial tension highly sensitive to solute concentration,

(6) low viscosities and diffusivities in both phases,

(7) absence of surface active agents, and

(8) interfaces of large extent ".

The mathematical procedure for the derivation of these stability criteria was based on a linear stability analysis and included the growth of small roll cells at a plane interface. Several assumptions and simplifications were made in this model, e.g. heat and density effects were not taken into account. However, it was suggested how to include heat effects in the analysis.

Comprehensive reviews of interfacial phenomena have been published by Sternling and Scriven (4), Sawistowski (5) and Berg (6).

Sternling and Scriven's work was later extended by Cho and Jones (7) who added heat effects due to heat of solution to the model. They concluded that Marangoni instabilities were dependent on the relative magnitude of the interfacial forces caused by temperature and concentration gradients and the directions of the heat and mass fluxes.

A further investigation of Marangoni instabilities in ternary systems, with the inclusion of heat effects was performed by Ortiz and Sawistowski (8) who concluded that thermal effects can only induce Marangoni instabilities when there is a release of heat at the interface in systems where the variation of interfacial tension with concentration and

temperature is negative. However, it was found that the order of magnitude of the temperature driven destabilising forces is normally too small to modify the stability criteria established by Sternling and Scriven.

Pearson (9) proposed a mechanism for thermal Marangoni instabilities to explain interfacial instabilities observed in thin films. According to his mathematical analysis thin films can show Marangoni instabilities when the thickness of the film is below a critical value.

Later, Ward and Brooks (10) explained the turbulence observed at an interface where mass transfer occurred, in terms of the interfacial effect of the heat of solution on the physical properties of the system.

The occurrence of Marangoni instabilities in binary liquid–liquid systems, i.e. systems in which the solute is also one of the phases, was considered theoretically impossible. In an isothermal binary system, if equilibrium is assumed to be reached instantaneously at the interface, the phase rule precludes any changes in interfacial concentrations. However, interfacial turbulence was observed experimentally by Merson and Quinn (11) in binary systems where the solute diffused into a radially moving interface. The authors interpreted the phenomena in terms of the Marangoni effect and suggested that interfacial tension gradients could be due either to interfacial concentration or temperature gradients caused by heats of solution.

Similar phenomena were observed by Austin, Ying and Sawistowski (12) who classified instabilities in binary systems into three types, according to the intensity of the instabilities:

(1) stable systems — diffusional mass transfer;

(2) unstable systems — weak instabilities: rippling and deformation of diffusional layer, slow movements;

(3) unstable systems — strong instabilities: violent movements.

Suggestions for the cause of the phenomena were heat effects due to heats of solution and values of the dynamic interfacial tension, as these may become very important during the relaxing time of the interface.

The classification of forty–six partially miscible binary systems according to an increasing order of intensity of turbulence was performed by Ying and Sawistowski (13) using Schlieren photography.

Anomalous values for mass transfer rates calculated for the binary system furfural/water was reported by Davies and Thornton (14). Although interfacial turbulence was hardly visible the increase in mass transfer rates was substantial and attributed to Marangoni instabilities caused by the heats of mixing.

Stability criteria for partially miscible binary systems were developed mathematically by Ortiz and Sawistowski (15) (16). Their linearised stability analysis indicated that a system is stable in both directions of transfer provided the heat of solution and the rate of change of interfacial tension with temperature are of the same sign and the kinematic viscosities of the two phases are approximately equal. Instabilities were predicted when mass transfer occurred out of the phase of higher viscosity.

Ortiz and Sawistowski stability criteria have been used by Hancock, White and Spruiell (17) to explain the occurrence of fingering and fluted void structures in wet spun fibres.

Aguirre, Klinzing, Chiang, Leaf and Minkoff (18) obtained temperature profiles for binary systems by numerically solving a diffusion model where they included the heat of solution and considered its non–linear relationship with concentration. Temperature difference predictions using this model

were to be found in agreement with experimental data from eight binary systems.

In a series of papers, Thornton and co–workers (19) (20) (21) report their quantitative investigations on the link between the rate of surface renewal due to Marangoni instabilities and mass transfer coefficients. By using a pendant drop they found that unless Marangoni instabilities were present there was no surface renewal. When Marangoni convection was observed mass transfer coefficients increased with the rate of surface renewal. Their experiments also showed that the rate of surface renewal decreased with surface age leading to time dependent mass transfer coefficients. Under the conditions of their experiments they suggested that this effect was not likely to be due to surface contamination but to transient changes in the interfacial region such as concentration variations in the layers adjacent to the interface.

Recently, Thornton and co–workers (22) (23) have proposed an equation for the mass transfer coefficients, derived from fundamentals, which includes the rate of surface renewal due to Marangoni instabilities. They have also discussed the importance of time dependent Marangoni instabilities on the generation of fresh surface in the design of high performance packed towers.

2.1.2 Systems with chemical reaction

In liquid–liquid systems, where mass transfer not only occurs by diffusion, but also by chemical reaction, the onset of Marangoni instabilities may be due to interfacial tension gradients created by changes in concentrations caused by the chemical reaction and/or heats of reaction.

In this section are included theoretical and experimental results reported in the literature for different systems and several types of chemical reactions.

Interfacial turbulence observed by Sherwood and Wei (24) in the extraction of acetic acid from an organic solvent into an alkaline solution was reported to be due to heat effects from the exothermal reaction. It was also found that interfacial turbulence was a strong function of solute concentration.

Heat effects were also reported to be the cause of the Marangoni instabilities observed by Thompson, Batey and Watson (25) in the transfer of nitric acid, uranyl–nitrate and plutonium nitrate from an aqueous to an organic phase. Interfacial oscillations had also been noticed by Lewis and Pratt (26) for the uranyl–nitrate system and they had also suggested that the phenomenon was related to the heat evolved during the transfer, i.e. heat of reaction.

In the extraction of uranium by TBP in kerosene, large irregular drops at the top of a pulsed column were observed by Batey, Lonie, Thompson and Thornton (27). The irregular behaviour was attributed to Marangoni phenomena.

A mechanism for the onset of interfacial convection for the extraction of uranyl–nitrate from an aqueous solution to an organic phase was proposed by Thompson and Perez de Ortiz (28). According to their linearised stability analysis of the system, the sign and magnitude of the interfacial tension variation with both concentration and temperature and the enthalpy of reaction are responsible for the onset of convection.

Pichugin, Tarasov, Arutiunyan and Goryachev (29) reported on the instabilities observed in the extraction of metals (lanthanides and some actinides) by di(2–ethylhexyl)phosphoric acid (DEPHA). The importance of

the concentration of extractant on the onset of interfacial turbulence is emphasized.

Spontaneous turbulence was also observed in the extraction of copper by a mixture of DEHPA and its sodium salt, DEPANa, by Nakache, Dupeyrat and Lemaire (30) who attributed the phenomena to Marangoni instabilities..

Nakache and Dupeyrat (31) (32) suggested that the turbulence observed in the reaction of an alkyl ammonium ion with KI, KBr and picric acid at an oil–water interface was due to Marangoni instabilities; the interfacial tension gradients were proposed to have been created by the oscillating reactions. Later, Nakache, Dupeyrat and Vignes–Adler (33) observed spontaneous motions at an interface between two immiscible liquids when a chemical reaction was present. The interface was kept at constant temperature and there was simultaneous transfer of two solutes, in opposite directions, one of them surface active. The notion of "assisted desorption" was introduced and defined as the "assistance" provided by an interfacial chemical reaction which transforms a very adsorbable species, e.g. a surfactant, into an easily desorbable one. The mechanism of instability proposed includes adsorption–desorption steps as well as diffusional, convective and chemical steps.

Another type of interfacial reaction was assumed in the studies by Steinchen and Sanfeld (34) (35). The conditions for the onset of instabilities when an autocatalytic reaction of the trimolecular type occurred at the interface between two immiscible liquids was analysed theoretically. It was suggested that the model studied could explain the deformation of biological cells upon the reception of a chemical message. A similar system has also been analysed by Deyhimi and Sanfeld (36).

Steinchen and Sanfeld (37) have also studied the motion induced by surface–chemical and electrochemical kinetics and given conditions for the onset of mechano–chemical instabilities.

The linear stability analysis of Steinchen and Sanfeld was extended by Hennenberg et al (38) to allow for any chemical reaction. The authors concluded that an unstable reaction may induce mechanical deformation of the interface and that although this may be a necessary condition, it is not a sufficient one because the chemical kinetics has to overcome the stabilizing effects of viscosities and densities.

A model for the stability behaviour of a fluid drop immersed in another fluid has been presented by Sorensen (39). Surface tension gradients are considered due to bulk diffusion or surface diffusion of surfactants and surface chemical reactions. This model predicts instabilities at low surface tensions and when diffusion of surfactants is from the exterior solution towards the inside of the drop. Importance is given to the application of the model to the understanding of several phenomena, e.g. detergency, tertiary oil recovery and cytologic phenomena in the living cell (chemotaxis, cell division and pseudope formation).

Theoretically, Ruckenstein and Berbente (40) applied a linear stability analysis to a system with a bulk chemical reaction of the first order. The authors found that the conditions for the occurrence of Marangoni instabilities are very sensitive even to small values of the reaction rate constant. However, general criteria could not be established.

2.2 Gravitational instabilities

Gravitational instabilities are due to density gradients which may have been started by temperature changes or volume contraction on mixing.

These instabilities were first observed at the beginning of this century by Benard (41), who observed regular cell patterns on a thin liquid layer heated from below. These phenomena, now also known as Benard instabilities were later studied mathematically by Rayleigh (42), who based his analysis on density stratification and derived a relation between viscous and buoyancy forces. This relation, the Rayleigh number, had to exceed a certain limiting value before any interfacial movements occurred. Benard cells could then be predicted using Rayleigh's quantitative criteria.

Later, Austin and Sawistowski (43) published an analysis for ternary systems, on the effects of density and direction of transfer on the gravitational stability of an interface. Their results are summarized in Table 2.1, where all the possible combinations of density and direction of transfer are presented.

The importance of the interaction between gravitational and diffusional processes was reported by Mel (44). The phenomena of "droplet sedimentation" in a continuous flowing system where an enzyme–substract reaction occurred was explained. He also mentions the importance of the lack of those instabilities in biological functions under a microgravity environment.

2.3 Combined Marangoni and gravitational instabilities

A liquid–liquid system may also show turbulence at the interface due to the combination of Marangoni and gravitational instabilities. This turbulence may be caused by the added effects of interfacial tension and density gradients at that interface. Therefore, the onset of Marangoni instabilities, for certain systems, can only be clearly understood when

gravitational effects can be considered negligible. Density gradients may be excluded from experimental conditions in Earth laboratories, by changing the compositions of the phases in the system to be studied, or by performing experiments in a microgravity environment. Microgravity conditions are achieved in orbiting laboratories, sounding rockets, drop towers or parabolic flights. Extensive work has been done in this field and some references are mentioned in this literature survey.

Research in convection phenomena in fluids heated from below was reviewed by Ostrach (45), who also pointed out the importance of the phenomena in the following fields: meteorology, astrophysics, aeronautics, chemical engineering, nuclear power and electronics.

Pearson (9), as previously mentioned, observed that under certain conditions the promotion of interfacial movements in some systems, was due to local changes in surface temperature which affected the surface tension. The mechanism of thermal instability, according to his mathematical analysis, is dependent on the thickness of the liquid layer: thinner films produce Marangoni type instabilities and deeper films buoyancy driven flows.

The importance of gravitational instabilities leading to surface renewal and to surface tension driven instabilities was later discussed by Austin (46) who investigated thirty-three binary systems and observed some very unstable interfaces in systems which exhibit volume contraction on mixing e.g. transfer of acetylacetone into water.

In ternary systems, the interaction between buoyancy and interfacial tension driven instabilities was investigated experimentally by Berg and Morig (47). Density differences were obtained by changing the composition of the phases. They concluded that when density forces were stabilising in a phase, convection was confined to a zone adjacent to the interface. When, according to Sternling and Scriven's stability criteria, convection

should have been present roll cells appeared which were damped and regenerated. When density forces were destabilizing, deep streamers were produced and convection in the form of roll cells was not present.

Experiments also performed with ternary systems, but under the microgravity conditions achieved in sounding rockets (Texus programme), were reported by Bruckner (48) (49). The results obtained were the ones predicted: less interfacial convection under microgravity than under gravitational conditions and violent interfacial convection was observed when the rocket was approaching the earth's surface.

The feasibility of producing dispersion alloys from binary systems with a miscibility gap was investigated by Walter (50). Results from experiments also conducted during the flight of Texus sounding rockets were reported. Under earth gravitational conditions, metallic dispersions are largely separated in their components due to sedimentation and buoyancy during cooling, through the miscibility gap. Under microgravity, samples were found with components largely separated. This separation, in the absence of buoyancy forces, is mostly attributed to Marangoni convection.

Fredriksson (51) has also studied, under microgravity, the effect of surface tension on the precipitation of droplets in immiscible alloys. Droplet movements caused by Marangoni convection produced a coarser structure of the alloy, due to collision of droplets. In low gravity these droplet movements become very important.

Also under microgravity conditions, Schwabe and Scharman (52) (53) (54) measured the critical Marangoni number for the transition point from laminar to oscillatory convection in a liquid bridge with free cylindrical surface (floating zone). They reported a critical Marangoni number of

approximately 10^4 and although the features of the oscillatory state of Marangoni convection seemed to be independent of gravity the critical Marangoni number (Ma) depends on the magnitude and direction of the buoyancy force.

In the German Spacelab Mission D1, Siekmann, Wozniak, Srulijes, Nahle and Neuhaus (55) carried out an experiment to observe bubble and drop motion induced by Marangoni convection. They concluded that for Marangoni numbers up to Ma = 300 and Reynolds number Re = 0.4, Marangoni convection could be applied for degasing of liquids under microgravity conditions. The authors also concluded that they found no indication that this type of convection could be used for the separation of liquid–liquid dispersions.

For most liquids, surface tension decreases with temperature. However, there are cases in which surface tension present extrema in their surface tension vs. temperature curves. In this category are included: liquid alloys, ceramics, some ionic surfactants and aqueous solutions of fatty alcohols. The influence on Marangoni convection for the case of a water/n–heptanol solution which shows a surface tension minimum was investigated by Legros, Limbourg–Fontaine and Petre (56) (57) and by Villers and Platten (58) (59). The latter authors studied experimentally, using a laser velocimetry technique, Marangoni and gravitational turbulence in a fluid confined in a rectangular horizontal cavity. A horizontal temperature gradient was imposed between the lateral walls of the cavity where the solution of water/n–heptanol was enclosed . Movements at the interface should be from cold to hot regions, but they proved that for different layer thicknesses the behaviour changes: gravitational convection is

favoured by thick layers and Marangoni convection by thin layers, which is in agreement with Pearson's mathematical analysis for thermal instabilities. For thicknesses of middle range two counter–rotating convective cells were observed.

A theoretical discussion of Marangoni and gravitational instabilities with emphasis on the role played by negative Rayleigh (Ra) and Marangoni (Ma) numbers was published by Lebon and Cloot (60). The authors concluded that surface tension gradients have destabilising effects when Ra and Ma are positive but they are stabilising when Ma is negative. When Ra and Ma are negative there is unconditional stability.

A numerical analysis of simulated unsteady Marangoni flows was performed by Napolitano, Golia and Viviani (61) and attention was focused on the time evolution of the velocity and temperature fields. This theoretical/numerical model is in good agreement with results from the Spacelab Mission D1 experiments, by the same authors (62).

It is interesting to mention some other published work in this field although it does not necessarily involve liquid–liquid systems.

The effects of non–uniform volumetric energy sources, temperature dependent viscosity and surface tension on Marangoni instabilities in a fluid layer, when a non–linear temperature profile is imposed from external incident radiation was recently investigated by Lam and Bayazitoglu (63). Critical conditions for the onset of the instabilities in a microgravity environment were determined using a linear stability analysis. It is concluded that the stability of the system depends on the sign of the viscosity variation with temperature; that the amount of heat generated internally in a phase, when external radiation is absorbed, is a destabilizing

effect while the degree of heat transfer from fluid to gas interface is a stabilizing factor.

Also recently, Oliver and Dewitt (64) demonstrated that irradiant heat may be exploited to induce droplet motion in a microgravity environment. The droplet was considered opaque and when it absorbed incident irradiant energy, temperature gradients were formed at the interface with consequent formation of interfacial tension gradients and droplet motion. An equation for the bulk droplet velocity is included and it is suggested that although the values predicted for the drop velocity are much smaller than those that would be important in most density gradient flows on earth, the surface tension driven velocities may be very significant in a microgravity environment.

The effects of a magnetic field and density on the critical Marangoni number and on the critical wave number in an electrically conducting horizontal liquid layer have been studied by Maekawa and Tanasawa (65). They found that the onset of Marangoni convection was suppressed by a magnetic field and that the distance between each convection cell became shorter as the magnetic field increased. A relation between critical Marangoni number and Rayleigh number was also derived.

Marangoni and gravitational convection were also investigated by Turner (66). He considered both gradients of temperature and concentration parallel to the body force direction, in order to explain some unusual phenomena such as salt finger and salt fountains in deep sea ocean.

In an experimental investigation Lee et al (67) studied fluid flows generated by natural convection due to the combined horizontal temperature and concentration gradients in rectangular enclosures. For the lower and

higher buoyancy ratios a unicell flow pattern was observed and for intermediate ranges of buoyancy ratio a multi–layer flow pattern was observed. For this regime they obtained interesting temperature and concentration profiles.

Gravitational stability			
Relative value of solute density	Dir. of transfer	Side A of interface	Side B of interface
$\rho_s<\rho_a<\rho_b$	A → B	stable	stable
	B → A	unstable	unstable
$\rho_a<\rho_s<\rho_b$	A → B	unstable	stable
	B → A	stable	unstable
$\rho_a<\rho_b<\rho_s$	A → B	unstable	unstable
	B → A	stable	stable

TABLE 2.1

CHAPTER 3

MARANGONI INSTABILITIES UNDER MICROGRAVITY

3.1 Mechanism of interfacial turbulence

Marangoni instabilities are interfacial flows caused by local variations of interfacial tension, which may be due to changes in interfacial concentrations, temperature, interfacial electrical charge or a combination of these.

A general simplified mechanism for Marangoni instabilities is represented in Figure 3.1 for a system where a solute S, which positively adsorbs at the interface, is transferred from Phase A to Phase B at steady state. If mass transfer is accompanied by heat effects temperature as well as concentration profiles will develop as shown in Figure 3.1a. For the sake of simplicity only the effect of variations of interfacial tension with concentration on interfacial stability will be discussed. A plot of interfacial tension vs concentration is also given in Figure 3.1a for the system under consideration.

Ever present small movements in the phases (Figure 3.1b) may bring fresh material from the bulk to the interface, thus changing locally the interfacial concentrations and producing interfacial gradients. For instance, if an eddy brings fresh solute from the bulk of Phase A into an interfacial Point 2, the renewed interface at that point will have a lower interfacial tension than the neighbouring Points 1 and 3. The interfacial tension gradient ($\gamma_i - \gamma_b$) causes a rapid spreading of material out of Point 2 at the interface (Figure 3.1c). This spreading motion compresses the adsorbed solute molecules at Points 1 and 3. Secondary interfacial tension gradients

are then created and the net change in solute concentration at Points 1 and 3 will depend on the ratio of viscosities and diffusivities of the two phases. Assuming that at Point 1 (and similarly at Point 3) the conditions will then be that $C_{A_1} > C_{A_2}$, i.e. $\gamma_1 < \gamma_2$, spreading will occur again but the movement will be in the opposite direction. This reverse movement may be either gentle, in which case it is damped and the system remains stable, or strong in which case turbulence will be observed in the form of eruptions. If the physical properties of the systems are such that $\gamma_1 > \gamma_2$, then the motion will continue in the form of roll cells. A thorough description of the mechanism of instabilities based on the role of the physical properties of different systems, is given by Sternling and Scriven (3).

As discussed in Chapter 2, Sternling and Scriven (3) derived criteria for the prediction of the onset of Marangoni instabilities for a single solute transferring between two immiscible phases, in the absence of heat effects. They also suggested a way to include heats of solution in their model. If the system is binary, i.e. one of the phases is also the solute and interfacial equilibrium is assumed to be attained instantaneously, under isothermal conditions the phase rule does not allow changes in interfacial concentrations, thus precluding the formation of any interfacial tension gradients. These systems should therefore be Marangoni stable. Experimentally, however, turbulence was observed by several workers (12) (14) who explained it in terms of either variations in interfacial tension due to temperature gradients caused by heats of solution or by dynamic changes of interfacial tension. Ortiz and Sawistowsky (15) (16) performed a stability analysis of binary liquid–liquid systems based on thermal Marangoni disturbances and developed stability criteria.

With reference to the temperature profiles in Figure 3.1 and taking into consideration the variation of γ with T in binary systems, the mechanism of thermal instability is similar to that caused by local changes in interfacial concentration. The eddies from the bulk create points with different interfacial temperatures leading to interfacial tension gradients. Spreading may lead to either interfacial stability or to sustained interfacial turbulence depending on the relative values of the physical properties, which now include the thermal diffusivities of the two phases.

The stability criteria previously mentioned for ternary and binary systems have been derived assuming negligible density effects. However, gravitational instabilities may also play an important role in the interfacial stability and may explain disagreements between predicted stability behaviour and experimental observations.

In binary systems, in particular, in which the proposed destabilizing mechanism is purely thermal, the relevance of gravitational effects on interfacial convection must be established since they may be the only destabilizing mechanism. Besides, in some of these systems there are substantial volume changes on mixing which could create unstable density gradients.

Gravitational instabilities due to volume contraction on mixing were reported by Austin (43) to be sufficient to cause interfacial instabilities. He also suggested that gravitational instabilities may lead to the onset of Marangoni instabilities, i.e. structured convection rather than random eddies may initiate Marangoni convection.

The interaction between the two types of instabilities when simultaneously present is very important as it may enhance interfacial turbulence (43) (47) (68).

Visually, Marangoni and gravitational instabilities are clearly different: gravitational instabilities are characterized by low frequency of motion and high depth of penetration, whereas in Marangoni instabilities the intensity of motion is high and the depth of penetration is low.

If thermal Marangoni disturbances were proved to be, on their own, strong enough to destabilize a liquid–liquid interface their effect could not be ignored in the mathematical stability analysis of extraction systems with interfacial chemical reaction, in which the heats of reaction could be an order of magnitude greater than the heats of solution.

Under normal gravitational conditions it is difficult to separate Marangoni from gravitational effects. However, if experiments were performed without gravity, only Marangoni instabilities could destabilize the interface, since convection due to unstable density gradients could not develop. In this way, Marangoni and gravitational instabilities could be decoupled.

Experiments under microgravity conditions can be conducted in orbiting spacelabs, drop towers, sounding rockets and parabolic flights. These facilities are available to European research workers through the European Space Agency (ESA). Thus a proposal was submitted to ESA for experiments on thermal Marangoni instabilities to be included in their ESA–NASA parabolic flights campaign in the United States.

3.2 Investigations under microgravity

The importance of the study of Marangoni instabilities under microgravity conditions has been widely recognized as shown by substantial number of investigations published in several areas, e.g. crystal growth from

melts and separation of immiscible alloys. However, up to now, the only publication related to solvent extraction is that of Bruckner's (48) (49) who, as mentioned in Chapter 2, reported experiments performed on ternary systems under the microgravity conditions achieved in sounding rockets.

The investigation of thermally driven interfacial turbulence in liquid–liquid binary systems under microgravity conditions has never been performed before. Thus, the purpose of this study was to decouple, under microgravity conditions, gravitational from thermal Marangoni instabilities in order to establish their relative importance in the onset and sustenance of interfacial convection.

The experimental work presented here was carried out in the microgravity environment provided by the NASA KC–135 parabolic flights in Houston, USA.

3.3 Selected systems

Binary systems are the only type of liquid–liquid systems in which Marangoni instabilities have been attributed to purely thermal effects. It has also been suggested that the interfacial turbulence observed in the extraction of uranyl–nitrate with tri–n–butylphosphate in odourless kerosene, a system with chemical reaction, may be also due to thermal Marangoni disturbances (28). However, due to safety restrictions on chemicals allowed on board the aeroplane, this system was not permitted to be flown.

The transfer of material from the organic to the aqueous phase was investigated for two binary systems: acetylacetone/water and ethylacetoacetate/water. The choice of these systems was based on their physical properties and the type of turbulence which had been previously

observed under gravity. Acetylacetone/water has been classified (12) as an unstable system with violent interfacial movements when the direction of transfer is from the organic to the aqueous phase; for the same direction of transfer, ethylacetoacetate/water shows weak instabilities (12). Both systems exhibit volume contraction on mixing, according to their physical properties which are shown in Table 3.1; thus they were both expected to exhibit gravitational instabilities.

The system acetylacetone/water was one of the systems selected by Ortiz and Sawistowski (16) to compare predicted and observed interfacial behaviour. The transfer of acetylacetone into water was predicted unstable. There are no predictions for the system ethylacetoacetate/water.

3.4 Parabolic flights

The trajectory of a KC–135 aeroplane while performing a parabolic flight is sketched in Figure 3.2. The parabola profile is executed from an altitude of 8,000 metres to an altitude of 11,000 metres. In the ascent the aeroplane flies with a 45^0 "nose high" angle, for 20 seconds, during which a 1.8–2.0 gravitational force is experienced. This is followed by a 25–30 seconds period of microgravity which is achieved by manoeuvring the free fall of the aeroplane just leaving the engines on to compensate for the effect of the air drag. A dive at a 45^0 angle follows and a 1.8–2.0 gravitational force is experienced again. The microgravity level achieved is $10^{-2} - 10^{-3}$. Figures 3.3 and 3.4 show the angles of the KC–135 while executing the descent (μ–g conditions) and the ascent (2–g conditions).

The experiments reported in this work were performed during three different parabolic flights. In each flight 25 parabolae were executed.

3.5 Experimental

3.5.1 Experimental set–up

Figure 3.5 shows a sketch and photograph of the experimental set–up which consisted of a frame on which the light source, photographic camera and test cell were mounted. The frame was made of aluminium and was bolted firmly into the aeroplane floor. Light was produced by an Olympus microscope lamp and the camera used was a Minolta 7000. This camera had a "computerised back" which provided the option of continuously photographing the subject at a preset time interval.

The purpose of this set–up was to allow the rays of light to cross the liquid–liquid interface and produce an image which was captured by the photographic camera. The use of a Schlieren system was considered, at first. However, the decision to use the set–up presented here was based on its compactness and the quality of the images obtained during experiments performed prior to the microgravity work.

Although the experimental set–up was very simple, the alignment and focusing of the light on the interface was a long and tedious procedure. A slight change in the incidence of the light on the interface can drastically modify the clarity of the photographs taken. It was also difficult to focus the camera on the interface, because the interface was only formed when the experiment commenced.

Two different types of cells were used as described in the following sections. In one cell the interface was flat and in the other a drop was formed.

3.5.1.1 Bicylindrical cell

Figures 3.6 and 3.7 show a schematic drawing and a photograph of the bicylindrical cell. This novel cell was specifically designed for the microgravity experiments performed in this work. Its main design characteristics were the following:

(i) the two phases were tightly separated before contact;

(ii) the cell could be filled leaving no air inside the chamber neither before nor after phases contact; this was thought to prevent phase mixing under gravity changes.

Using this design two cells were constructed: one made of brass and the other made of stainless steel. In both cases the body of the cell was cylindrical and had a cylindrical extension which enclosed a PTFE rod containing one of the liquid chambers. This "piston like" rod could be pushed into alignment with the top chamber which was located in the main body of the cell. Two windows made of optical glass allowded photographs to be taken in a direction perpendicular to the interface.

During the experiments, a flat interface was formed between the two liquid phases by pushing the "piston like" chamber containing the aqueous phase into contact with the organic phase which was contained in the top chamber.

A shortfall of this cell design is that despite a careful, slow, pushing movement of the "piston" there was always a slight initial perturbation of the interface due to shear stresses.

3.5.1.2 Drop cell

Figure 3.8 shows a photograph of the drop cell. It consists of a stainless steel cell with two rectangular Schlieren glass windows. A syringe

with a stainless steel needle could be inserted at the top of the cell. A drop of the organic phase was formed at the end of the stainless steel needle and suspended in the aqueous phase contained in the cell.

3.5.2 Experimental procedure

The organic phases were pre–saturated with water so that the only mass transfer observed was from the organic phase into the water.

A fresh interface, between the organic and the aqueous phase, was formed and photographed in gravity environment and the same operation performed under microgravity. In some experiments, the same interface was continuously photographed under microgravity and while gravity environment was re–established.

3.6 Results and discussion

The duration of the microgravity period for each parabola was 25–30 seconds. Although short, this period was long enough to observe the effect of microgravity on the interfacial behaviour of the two systems studied. During the three flights, depending on the weather conditions and the pilot's abilities, there were fluctuations in the level of microgravity. An example of this may be seen in Figure 3.9, for one parabola.

Many photographs were taken some of which were selected to be discussed in this chapter.

Each binary system investigated will now be considered, in turn, in the next two sections.

3.6.1 Acetylacetone/water

Figure 3.10 shows a sequence of frames, taken at 2 second intervals, of a drop of acetylacetone in water under gravity conditions. Marangoni instabilities were observed in the form of eruptions, quite close to the surface of the drop (frame 1), which develop into streams (gravitational instabilities) due to density differences (frames 2 and 3). The turbulence observed lasted for several minutes.

A sequence of frames, taken at 1 second intervals under microgravity, is shown in Figure 3.12. Turbulence is confined to the area surrounding the drop and has almost disappeared after 8 seconds. A decrease in Marangoni turbulence with time has been reported by Rogers, Thompson and Thornton (69), and Javed, Thornton and Anderson (23), for suspended aqueous drops in organic phases. They suggest that this decrease may be due to accumulation of solute in the interfacial region with the consequent decrease in mass transfer driving force and/or to interfacial ageing effects.

Similarly, using the bicylindrical cell under gravity conditions, the photograph of the flat interface in Figure 3.13 shows small convection cells surrounded by larger ones. Under microgravity the same system shows small convection cells, which seem to indicate that they were due to Marangoni instabilities, while larger cells resulted only from the combined effect of Marangoni and gravitational instabilities.

The observation of this system under microgravity conditions indicates the onset of instabilities in the absence of gravity.

Therefore, in microgravity, interfacial tension gradients caused by temperature differences at the interface are, for the acetylacetone/water system, strong enough to initiate and sustain interfacial turbulence. The

increase in duration and intensity of the instabilities under a gravity environment might be due to an increase in the rate of surface renewal caused by gravitational instabilities. The interaction between the two types of instabilities may be an additional factor for the difference in interfacial behaviour under microgravity and gravity environments.

It may then be concluded that the acetylacetone/water system:

(i) is unstable with respect to Marangoni instabilities in the absence of gravitational instabilities;

(ii) that gravitational instabilities not only enhance turbulence, as expected, but also sustain it for a longer period;

(iii) and that Marangoni instabilities do not need to be triggered by gravitational instabilities.

3.6.2 Ethylacetoacetate/water

Figure 3.11 shows a sequence of frames taken at 2 second intervals under gravity conditions. Figure 3.14 shows a sequence of frames taken at 1 second intervals under microgravity. The drop in the second series of photographs was continuously photographed, throughout and into the re-establishment of a gravity environment, as may be seen in Figure 3.15.

It is worth mentioning that because of the difference in the densities of the two phases, it is easier to observe the system when the drop of the more dense phase, i.e. ethylacetoacetate, is injected upwards.

While photographing the sequence in Figure 3.15, a large air bubble was created at the top of the drop. Air bubbles, which under microgravity were randomly distributed within the drop (see Figure 3.14), moved to the top of the drop once the gravity environment was re-established.

This system has been classified (12) as presenting weak instabilities under normal gravity conditions. From the photographs taken, it may be concluded, that in microgravity, this system hardly showed any interfacial convection. However, when a gravity environment was re–established the system became turbulent.

From the observation of the behaviour of the ethylacetoacetate/water system under microgravity, it may be concluded that density gradients, either due to volume contraction or temperature gradients, seem to be the cause of the onset of the instabilities observed in a gravity environment.

There is no theoretical prediction for the stability of this system with respect to Marangoni disturbances. It would be interesting to know its heats of solution so that the criteria proposed by Ortiz and Sawistowski could be used to predict the interfacial behaviour of this system. Unfortunately values for the heats of solution are not available. If the heats of solution were such that the system were predicted unstable, perhaps stagnant layers of material at the interface would prevent any manifestation of interfacial turbulence until gravitational instabilities penetrated through that barrier. If the system were predicted Marangoni stable, then the turbulence observed under gravitational conditions would be purely gravitational.

3.7 Conclusions

The conclusions obtained from the observations of the two binary liquid–liquid systems under microgravity are as follows:

Temperature gradients alone are sufficient to induce interfacial tension gradients that initiate Marangoni instabilities. Once initiated they were of

shorter duration than instabilities developed under gravitational conditions. Gravitational instabilities, when present, enhanced the rate of surface renewal, thus helping to sustain interfacial convection.

The above conclusions indicate that if thermal Marangoni disturbances are strong enough to destabilize binary systems they could also induce instabilities in systems with heats of reaction.

For the ethylacetoacetate/water system the instabilities were very weak and hardly visible under microgravity. Values for the heats of solution have not been found in the literature, thus making it impossible to use stability criteria to predict the interfacial behaviour of this system. Therefore, the system is either only gravitationally unstable or, if Marangoni unstable, instabilities have to be initiated by gravitational flows.

	$\rho^{25°c}_{pure}$ (kg m^{-3})	$\rho^{25°c}_{saturated\ water}$ (kg m^{-3})
water	997.0 (*)	————
acetylacetone	972.0 (*)	1001.3 (***)
ethylacetoacetate	1030.0 (*)	1000.6 (**)

TABLE 3.1

(*) Handbook of Chemistry and Physics

(**) Institution of Chemical Engineers, PPDS service

(***) Austin (46)

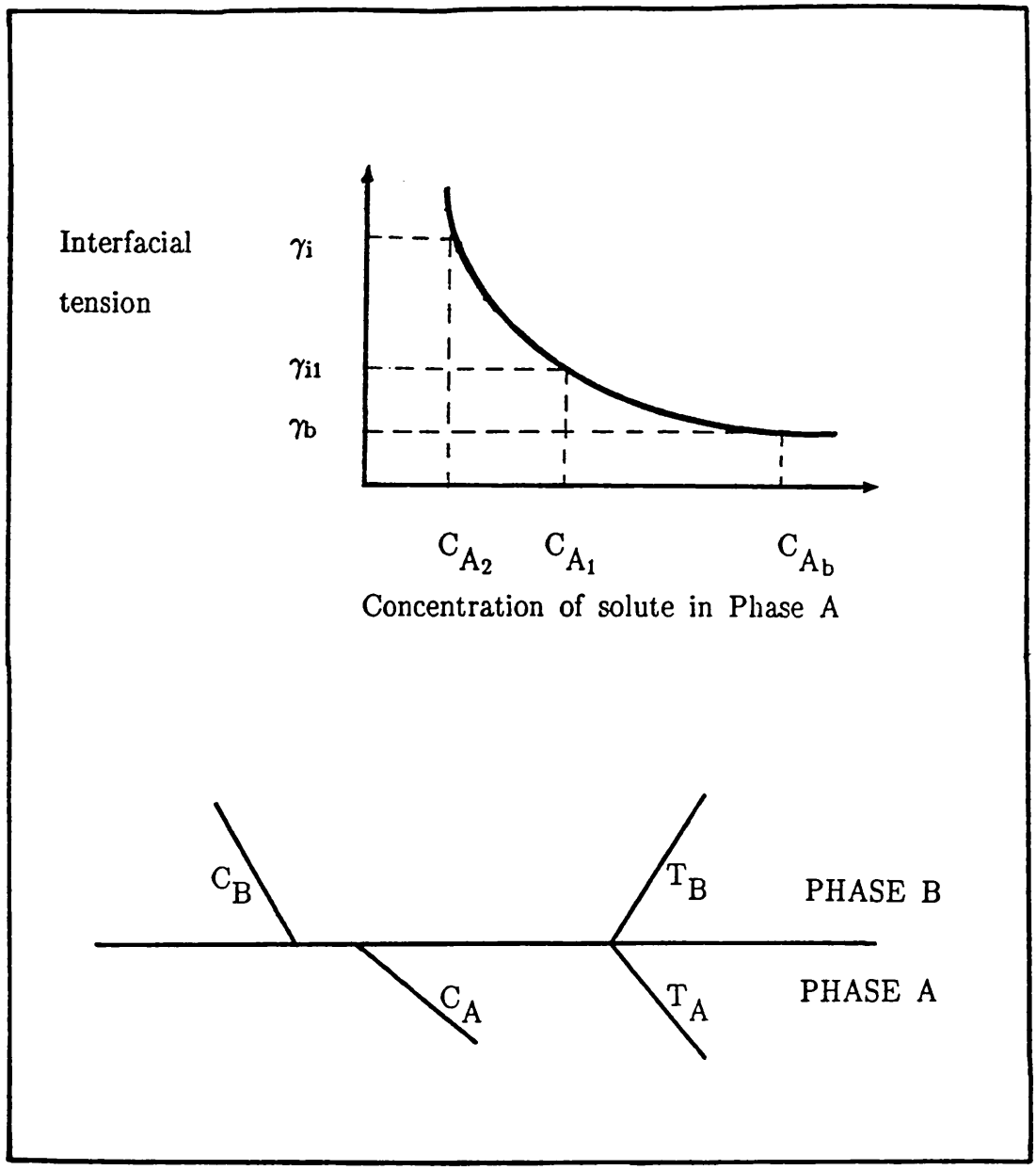
Interfacial
tension
γ_i
γ_{i1}
γ_b
C_{A_2}
C_{A_1}
C_{A_b}
Concentration of solute in Phase A
C_B
T_B
PHASE B
C_A
T_A
PHASE A

FIGURE 3.1a

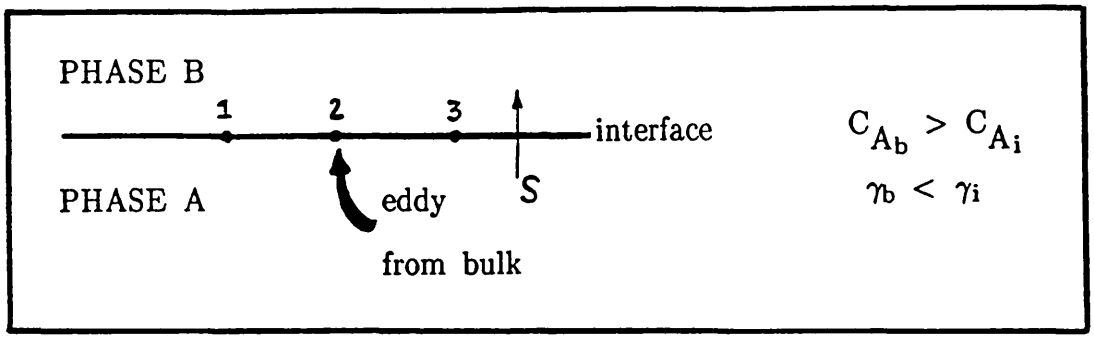

FIGURE 3.1b

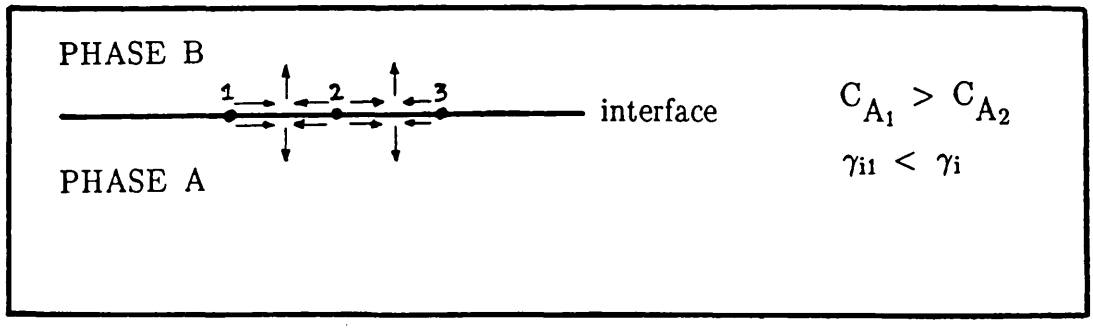

FIGURE 3.1c

Mechanism of interfacial turbulence

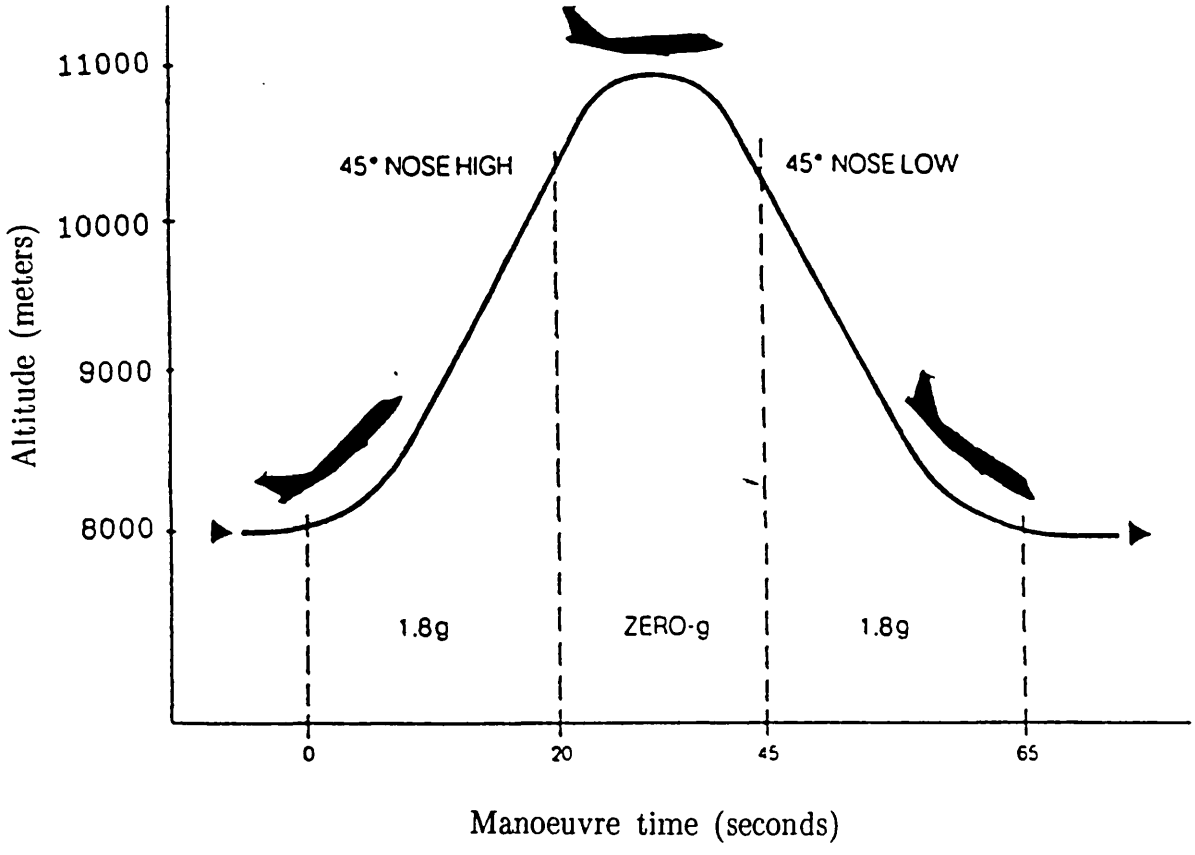

FIGURE 3.2

Manoeuvre profile during parabola

FIGURE 3.3

Descent (μ–g conditions)

FIGURE 3.4

Ascent (1.8 – 2 g conditions)

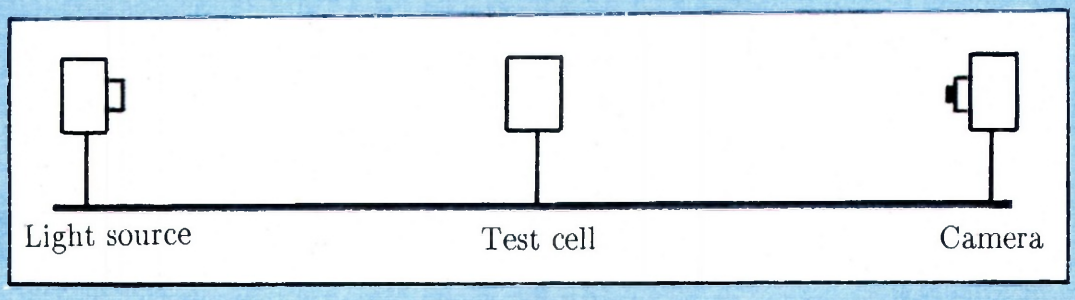

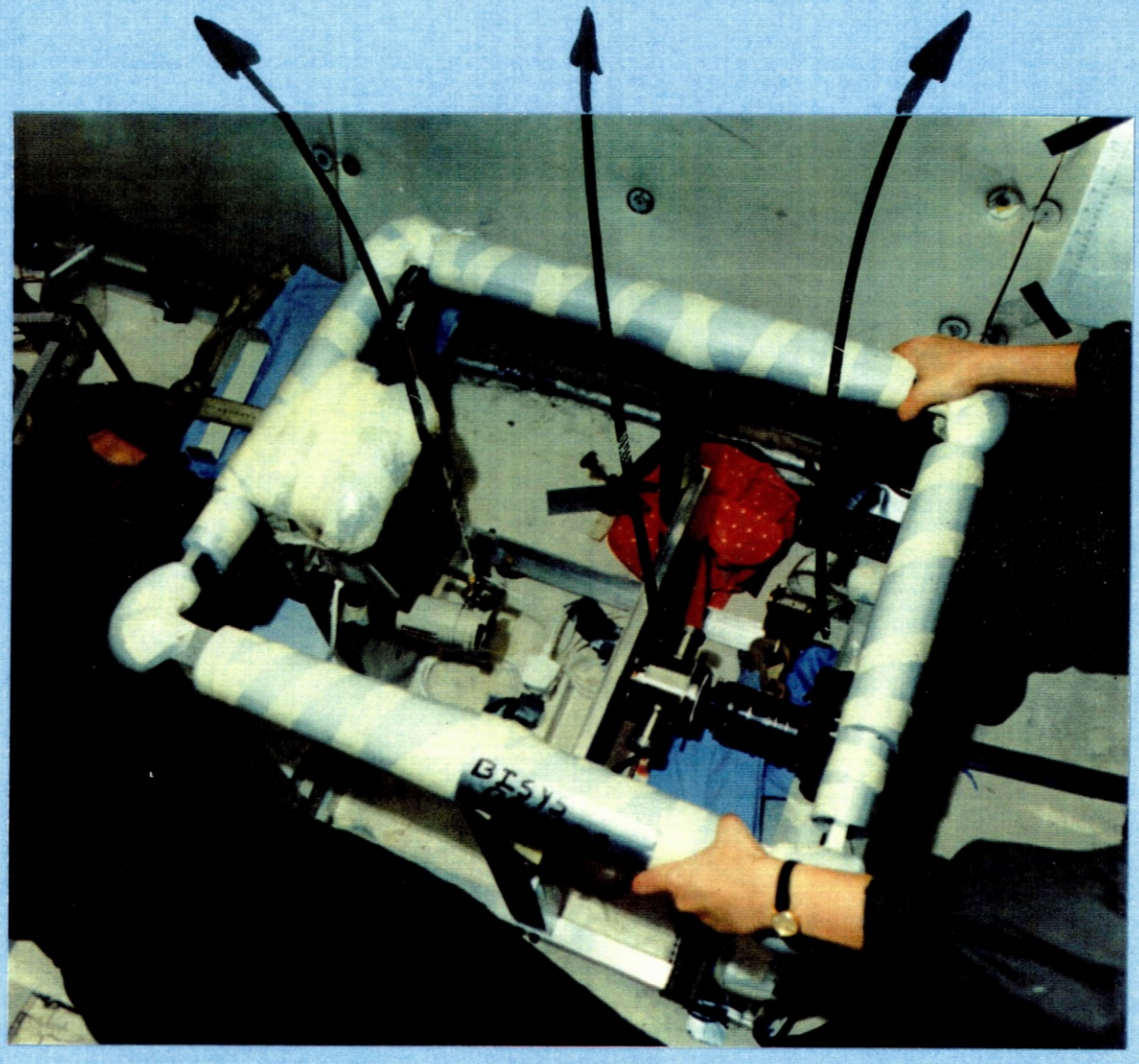

FIGURE 3.5

Experimental set–up

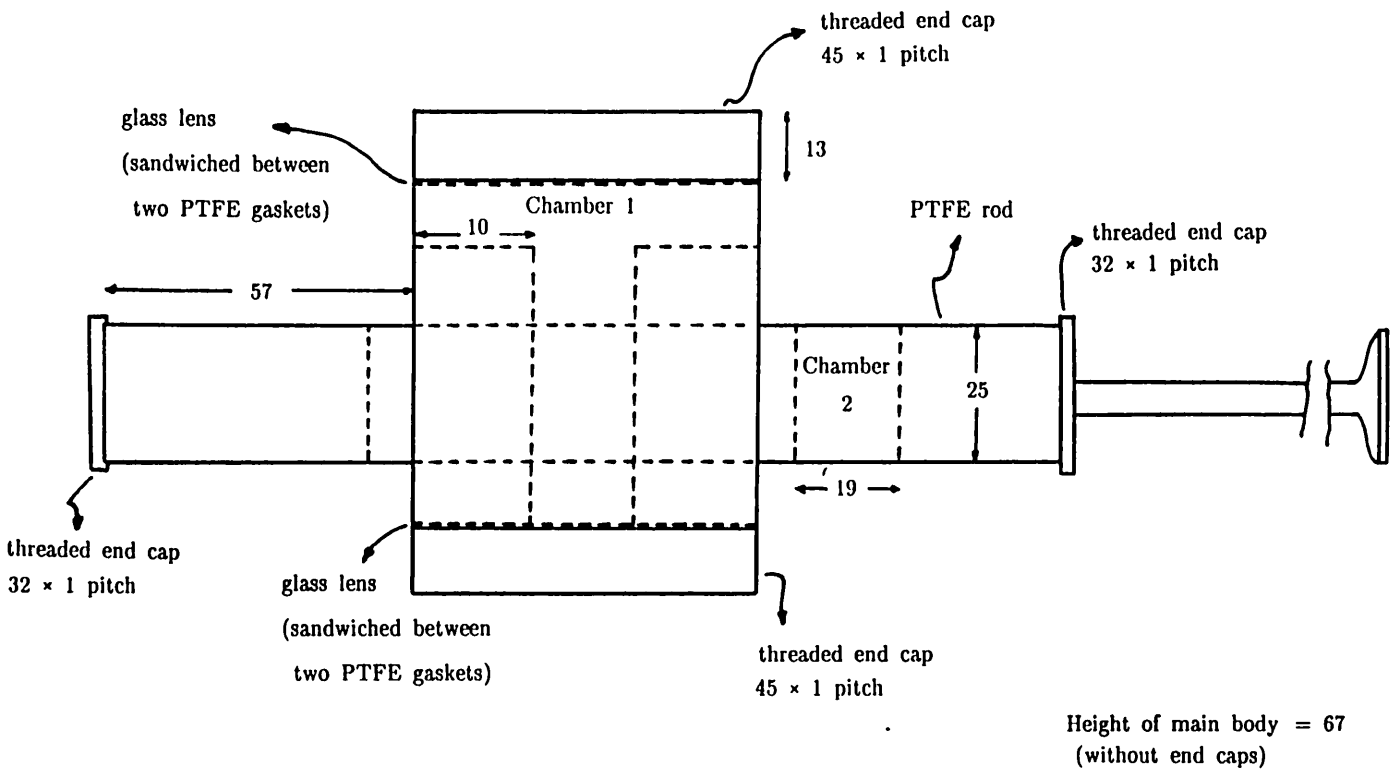

FIGURE 3.6

Schematic drawing of the bicylindrical cell

(all dimensions in mm)

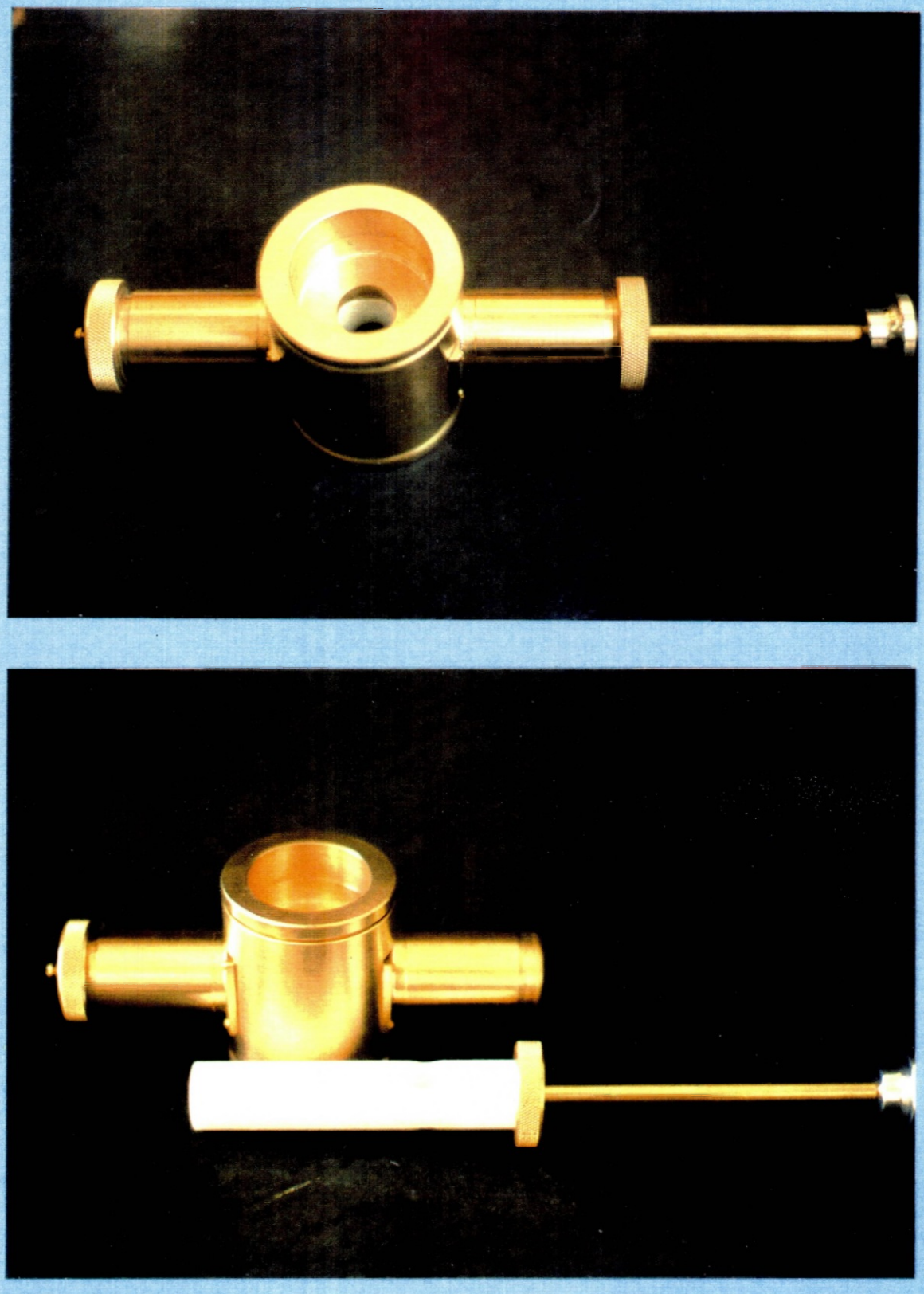

FIGURE 3.7a

View of the bicylindrical cell

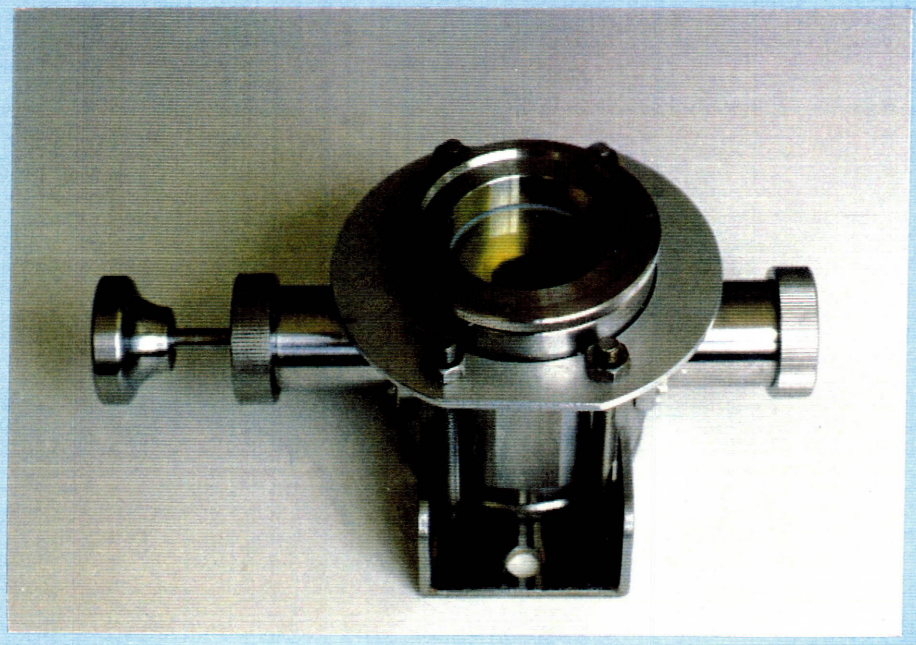

FIGURE 3.7b

View of the assembled bicylindrical cell

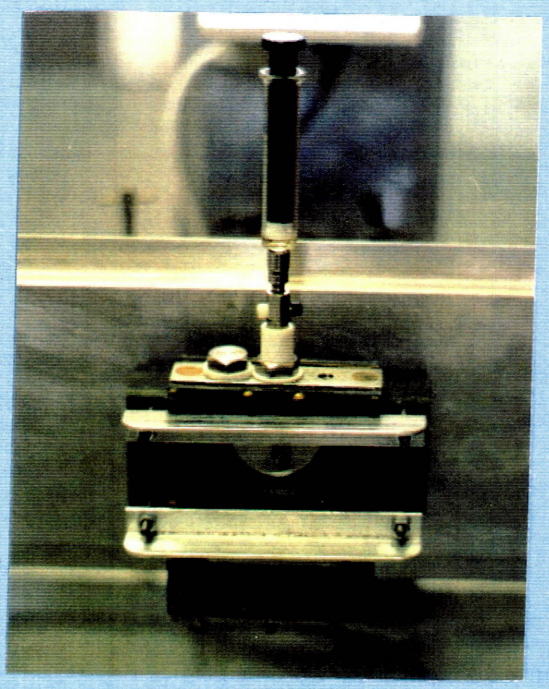

FIGURE 3.8

View of the assembled drop cell

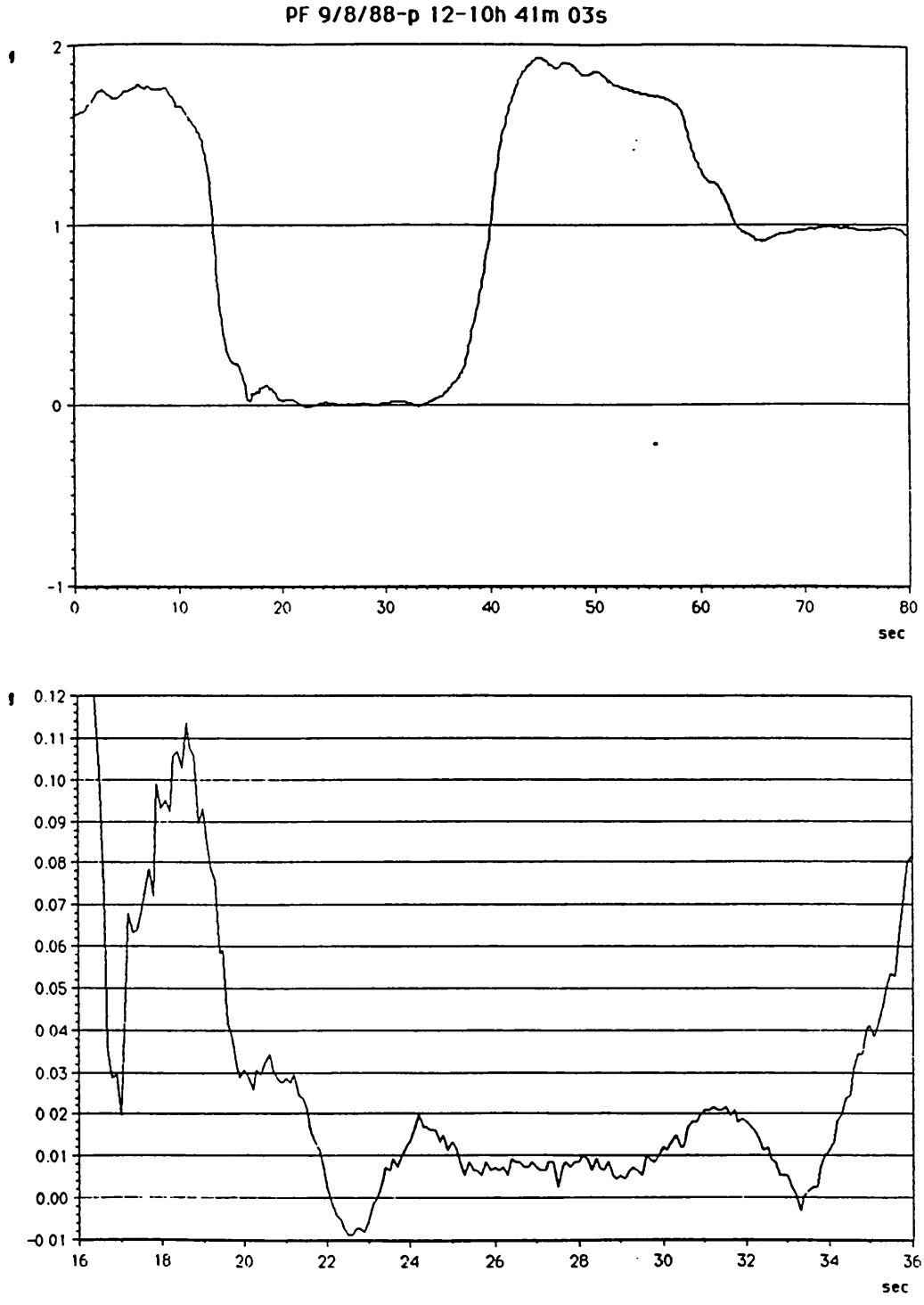

FIGURE 3.9

Example of a plot of the microgravity level during a parabola

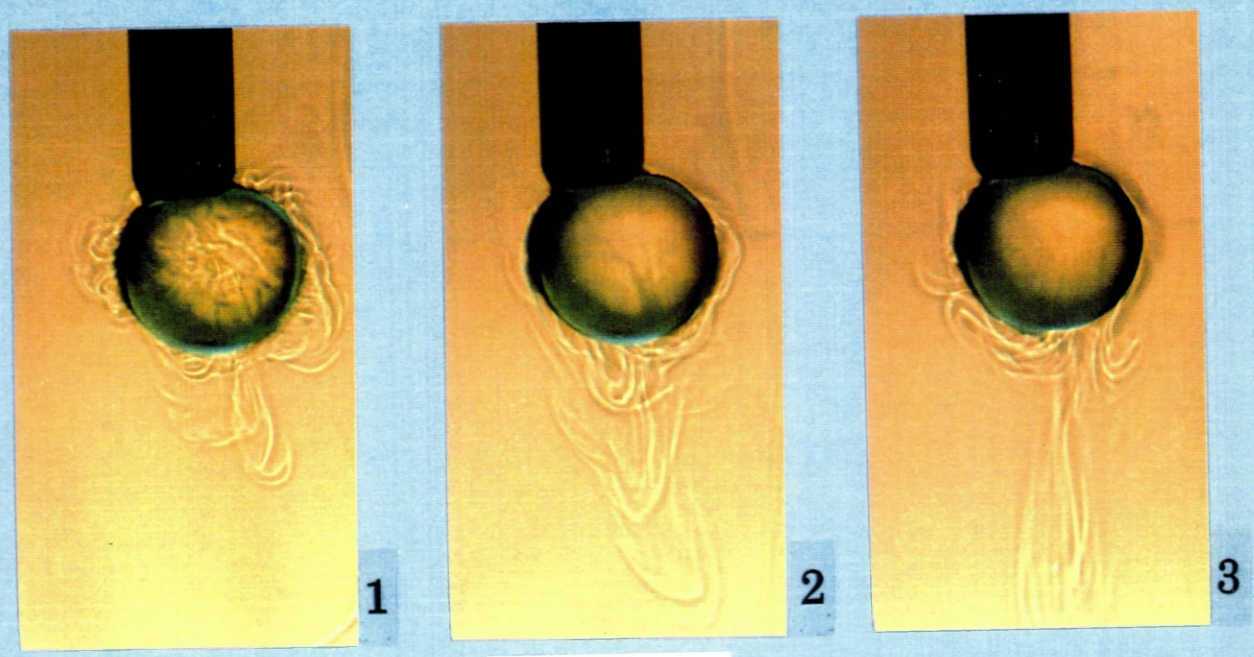

FIGURE 3.10

Acetylacetone-Water

(1-g)

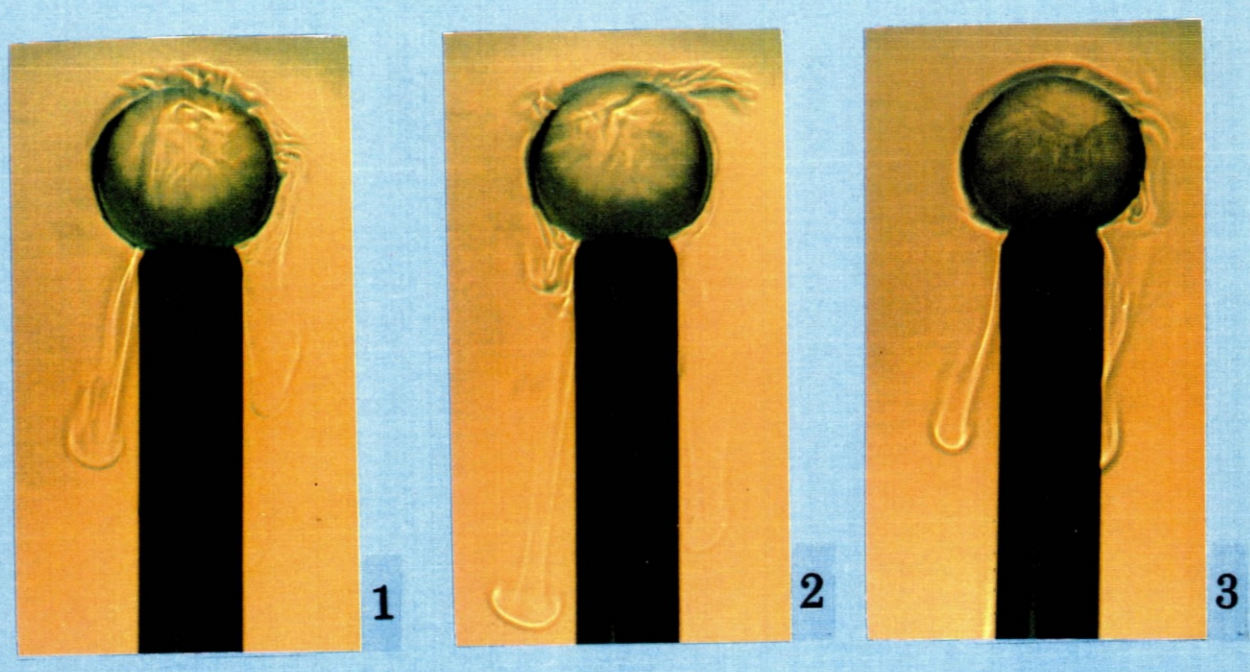

FIGURE 3.11

Ethylacetoacetate-Water

(1-g)

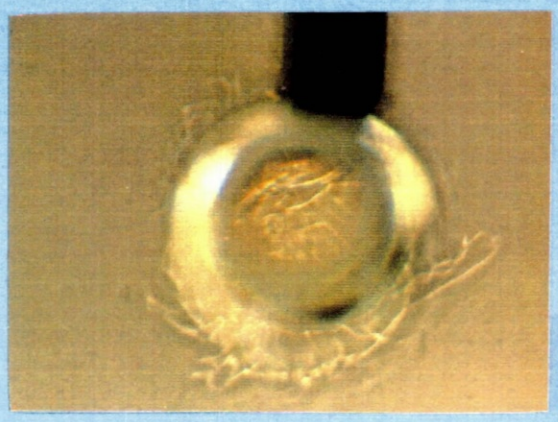
1

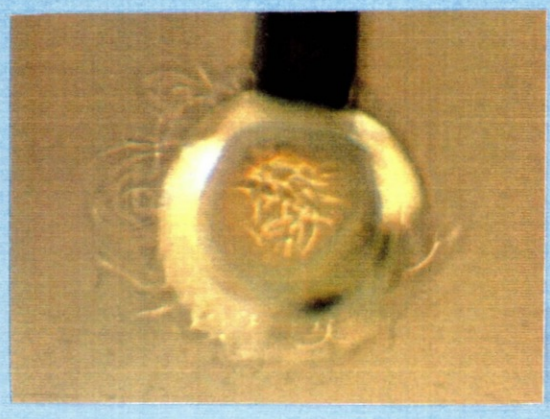
2

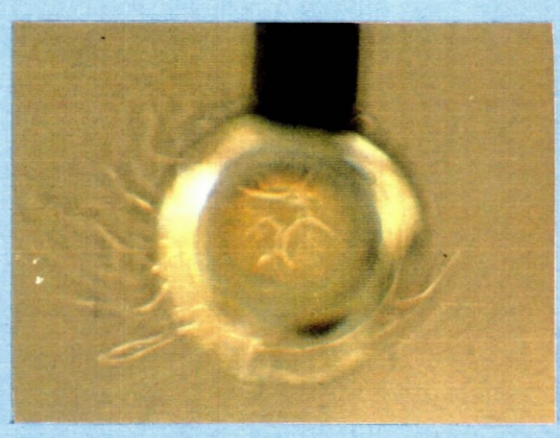
3

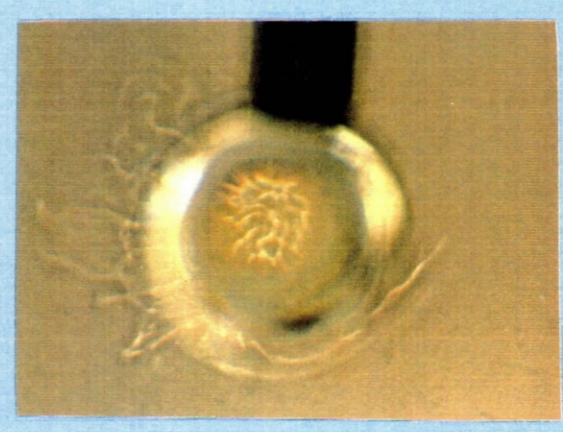
4

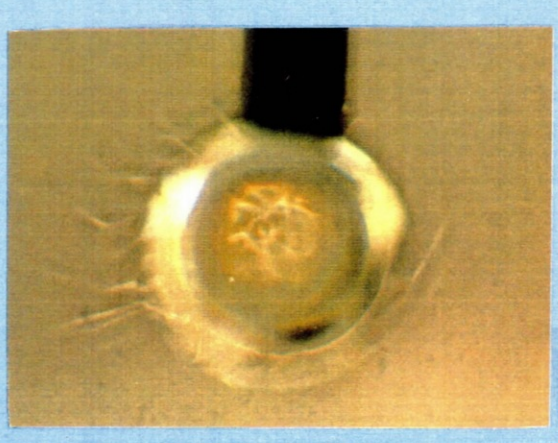
5

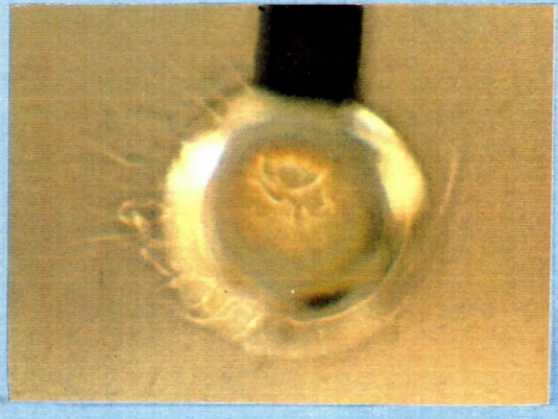
6

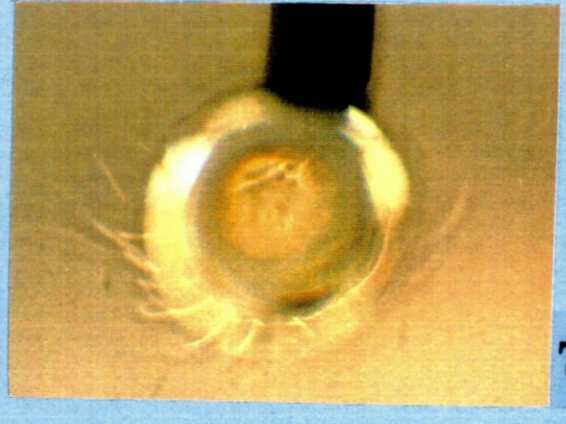
7

FIGURE 3.12

Acetylacetone-Water

(μ-g)

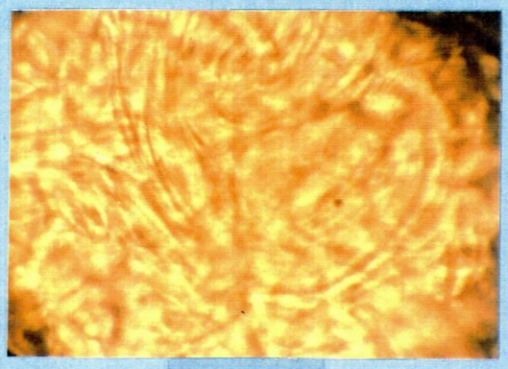

(1-g)

(μ-g)

FIGURE 3.13

Acetylacetone - Water

FIGURE 3.14

Ethylacetoacetate - Water

(μ-g)

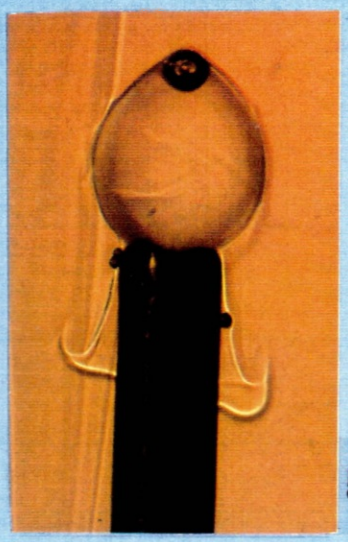
5


6


7

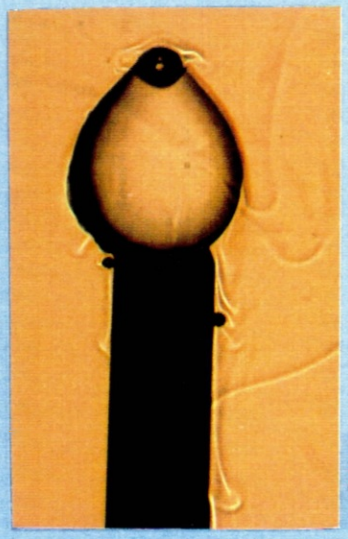
8

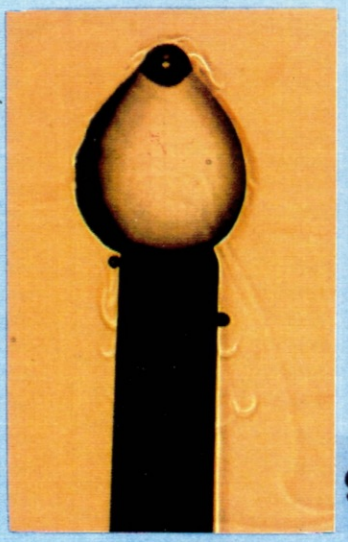
9

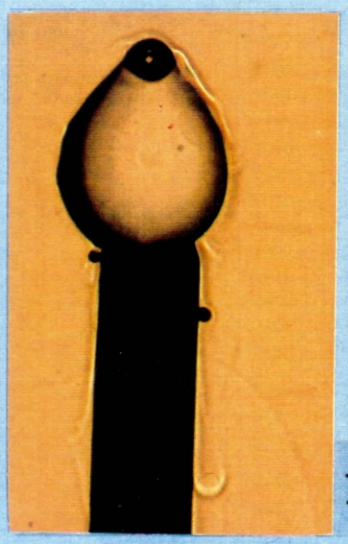
10


11

FIGURE 3.15

Ethylacetoacetate-Water

(g-environment)

CHAPTER 4

MATHEMATICAL ANALYSIS

4.1 Introduction

In this chapter a mathematical stability analysis is applied to a system which consists of two immiscible liquid phases with a reversible chemical reaction occurring at the interface.

The procedure presented in this work follows the linear stability analysis used by Sternling and Scriven (3) in their study of Marangoni instabilities in a liquid–liquid system with diffusional mass transfer.

The mathematical description of the unperturbed system entails the combination of the equations of motion, molecular diffusion and chemical reaction with and without heat effects. Perturbations are then introduced in these equations that lead to a characteristic equation which describes the evolution of the perturbation with time.

In this chapter a characteristic equation for the case of an isothermal system is obtained and conditions are given for the development of a characteristic equation for a system with heat effects.

The mathematical manipulation of terms was performed using an Amdahl computer and the software package "REDUCE". Computer programs written for the algebraic development of the theoretical equations, for the isothermal case, are included in Appendix A.

4.2 Linear stability analysis

The model studied is a two–dimensional configuration of two semi–infinite immiscible liquid phases in contact along a plane interface.

The phases are in thermal equilibrium and there is a chemical reaction at the interface. A very simplified form of a chemical reaction has been considered and is represented by

$$A + B \rightleftharpoons P$$

The interfacial chemical reaction is assumed to be a pseudo–first order reversible reaction, thus the flux is given by

$$N_a = k'_1 C_a - k_2 C_p$$

The chemical reaction may or may not be accompanied by heats of reaction and the concentration and temperature profiles are assumed independent of time. The concentration of B (extractant) is considered in excess. A schematic drawing of the concentration and temperature profiles are shown in Figure 4.1.

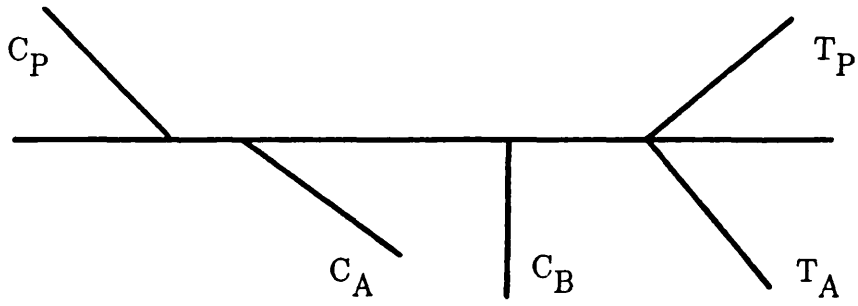

FIGURE 4.1

The system is initially undisturbed and an analysis is to be made of the response of the system when two–dimensional infinitesimal disturbances are introduced. When the disturbances grow with time, the system is unstable and when they decay the system is stable.

4.2.1 Equations of motion

The Navier–Stokes equations for an incompressible Newtonian fluid in the absence of body forces and for two–dimensional flow are

$$\frac{\partial u}{\partial t} + u\frac{\partial u}{\partial x} + v\frac{\partial u}{\partial y} = -\frac{1}{\rho}\frac{\partial p}{\partial x} + \nu\left(\frac{\partial^2 u}{\partial x^2} + \frac{\partial^2 u}{\partial y^2}\right) \qquad (4.1)$$

$$\frac{\partial v}{\partial t} + u\frac{\partial v}{\partial x} + v\frac{\partial v}{\partial y} = -\frac{1}{\rho}\frac{\partial p}{\partial y} + \nu\left(\frac{\partial^2 v}{\partial x^2} + \frac{\partial^2 v}{\partial y^2}\right) \qquad (4.2)$$

The system is initially quiescent (creeping flow) therefore the non–linear terms in Equations (4.1) and (4.2) may be neglected and the pressure terms may be eliminated by cross–differentiation.

Subtracting Equation (4.1) from Equation (4.2)

$$\frac{\partial^2 v}{\partial t\,\partial x} - \frac{\partial^2 u}{\partial t\,\partial y} = \nu\left[\frac{\partial^3 v}{\partial x^3} + \frac{\partial^3 v}{\partial x\,\partial y^2} - \frac{\partial^2 u}{\partial x^2\,\partial y} - \frac{\partial^3 u}{\partial y^3}\right] \qquad (4.3)$$

Introducing a stream function Ψ

$$u = -\frac{\partial \Psi}{\partial y} \quad \text{and} \quad v = \frac{\partial \Psi}{\partial x} \qquad (4.4)$$

so that the continuity equation

$$\frac{\partial u}{\partial x} + \frac{\partial v}{\partial y} = 0 \qquad (4.5)$$

is satisfied, Equation (4.3) becomes

$$\frac{\partial^3 \Psi}{\partial t \partial x^2} + \frac{\partial^3 \Psi}{\partial t \partial y^2} = \nu \left[\frac{\partial^4 \Psi}{\partial x^4} + 2 \frac{\partial^4 \Psi}{\partial x^2 \partial y^2} + \frac{\partial^4 \Psi}{\partial y^4} \right] \qquad (4.6)$$

A solution for Ψ in Equation (4.6) will be assumed to be of the form

$$\Psi = \varphi(x)\, e^{i\alpha y}\, e^{\beta t} \qquad (4.7)$$

where: ψ is the x–component of the perturbation; $\alpha = 2\pi/\lambda$ is the wavenumber; λ is the wavelength and β is the growth constant of the perturbation.

Substituting Equation (4.7) into Equation (4.6) the Orr–Sommerfeld equation is obtained for a two–dimensional disturbance in an initially quiescent medium,

$$\varphi'''' - 2\,\alpha^2\,\varphi'' + \alpha^4\,\varphi = \frac{\beta}{\alpha^2 \nu}\,(\alpha\ \varphi'' - \alpha^4\,\varphi) \qquad (4.8)$$

A new variable $X = \alpha x$ may be introduced to simplify Equation (4.8) which then becomes

$$\varphi'''' - 2\,\varphi'' + \varphi = \frac{\beta}{\alpha^2 \nu}\,(\alpha^2\,\varphi'' - \alpha^4\,\varphi) \qquad (4.9)$$

The solution for Equation (4.9) when $\beta \neq 0$ is

$$\varphi = A_1 e^x + A_2 e^{-x} + A_3 e^{px} + A_4 e^{-px} \qquad (4.10)$$

and for $\beta = 0$

$$\varphi = A_5 e^x + A_6 e^{-x} + A_7 x e^x + A_8 x e^{-x} \qquad (4.11)$$

where $p = \sqrt{1 + \frac{\beta}{\alpha^2 \nu}}$ and the constants A_1 to A_8 have to be evaluated from boundary conditions.

4.2.1.1 Assumptions and boundary conditions

It is assumed that:

— the interfacial tension is sufficiently high for the interface to keep planar;

— the disturbance stays finite at large distances from the interface (boundary conditions (1) to (4));

— the interface (x=0) is a streamline (boundary conditions (5) and (6));

— there is no slip at the interface (boundary condition (7));

— there is continuity of tangential stress at the interface (boundary condition (8));

These assumptions may be expressed in the following boundary conditions:

(1) $u_p(\infty) = 0$

(2) $u_a(-\infty) = 0$

(3) $v_p(\infty) = 0$

(4) $v_a(-\infty) = 0$

(5) $u_p(0,y,t) = 0$

(6) $u_p(0,y,t) = u_a(0,y,t)$

(7) $v_p(0,y,t) = v_a(0,y,t)$

(8) $\tau_{xya} - \tau_{xyp} = \frac{\partial \sigma_{yy}}{\partial y}$

4.2.1.2 Hydrodynamic boundary conditions

To calculate the constants in Equations (4.10) and (4.11) the above boundary conditions may be redefined using Equations (4.4) and (4.7):

(1) $\varphi_p(\infty) = 0$

(2) $\varphi_a(-\infty) = 0$

(3) $\varphi_p'(\infty) = 0$

(4) $\varphi_a'(-\infty) = 0$

(5) $\varphi_p(0) = 0$

(6) $\varphi_a(0) = 0$

(7) $\varphi_p'(0) = \varphi_a'(0)$

(8) $\tau_{xya} - \tau_{xyp} = \frac{\partial \sigma_{yy}}{\partial y}$ at $x = 0$

The shear stresses on each side of the interface are defined as:

$$\tau_{xyp} = \mu_p \left(\frac{\partial u_p}{\partial y} + \frac{\partial v_p}{\partial x}\right) = \mu_p \left(\frac{\partial^2 \Psi_p}{\partial x^2} - \frac{\partial^2 \Psi_p}{\partial y^2}\right) \qquad (4.12)$$

$$\tau_{xya} = \mu_a \left(\frac{\partial u_a}{\partial y} + \frac{\partial v_a}{\partial x}\right) = \mu_a \left(\frac{\partial^2 \Psi_a}{\partial x^2} - \frac{\partial^2 \Psi_a}{\partial y^2}\right) \qquad (4.13)$$

The dynamic interfacial tension σ_{yy}, according to the Boussinesq formulation (70), depends on the rate of deformation of the interface:

$$\sigma_{yy} = \sigma_0 + \kappa \left(\frac{\partial v}{\partial y} + \frac{\partial w}{\partial z}\right) + \Gamma \left(\frac{\partial v}{\partial y} - \frac{\partial w}{\partial z}\right) \text{ at } x = 0 \quad (4.14)$$

$$\sigma_{yy} = \sigma_0 + \mu \left(\frac{\partial v}{\partial y}\right) = \sigma_0 + \mu_s \left(\frac{\partial^2 \Psi}{\partial x \partial y}\right) \text{ at } x = 0 \quad (4.15)$$

and

$$\frac{\partial \sigma_{yy}}{\partial y} = \frac{\partial \sigma_0}{\partial y} + \mu_s \left(\frac{\partial^3 \psi}{\partial x \partial y^2}\right) \quad (4.16)$$

Considering the static interfacial tension as a function of the concentrations of the two components and temperature,

$$\frac{\partial \sigma_0}{\partial y} = \frac{\partial \sigma_0}{\partial C_a} \frac{\partial C_a}{\partial y} + \frac{\partial \sigma_0}{\partial C_p} \frac{\partial C_p}{\partial y} + \frac{\partial \sigma_0}{\partial T} \frac{\partial T}{\partial y} \quad (4.17)$$

and substituting Equation (4.17) in Equation (4.16)

$$\frac{\partial \sigma_{yy}}{\partial y} = \left(\frac{\partial \sigma_0}{\partial C_a} \frac{\partial C_a}{\partial y} + \frac{\partial \sigma_0}{\partial C_p} \frac{\partial C_p}{\partial y} + \frac{\partial \sigma_0}{\partial T} \frac{\partial T}{\partial y}\right) + \mu_s \left(\frac{\partial^3 \psi}{\partial x \partial y^2}\right) \quad (4.18)$$

After the substitution of Equations (4.12), (4.13) and (4.18) into boundary condition (8), this becomes

$$\left(\frac{\partial \sigma_0}{\partial C_a} \frac{\partial C_a}{\partial y} + \frac{\partial \sigma_0}{\partial C_p} \frac{\partial C_p}{\partial y} + \frac{\partial \sigma_0}{\partial T} \frac{\partial T}{\partial y}\right) + \mu_s \left(\frac{\partial^3 \psi}{\partial x \partial y^2}\right) =$$

$$= \mu_a \left(\frac{\partial^2 \Psi_a}{\partial x^2} - \frac{\partial^2 \Psi_a}{\partial y^2}\right) - \mu_p \left(\frac{\partial^2 \Psi_p}{\partial x^2} - \frac{\partial^2 \Psi_p}{\partial y^2}\right) \quad (4.19)$$

Using boundary conditions (1) to (6), for $\beta \neq 0$

$$\varphi_P = A_2 \, (e^{-x} - e^{-p_P x}) \qquad \text{for } x \geq 0 \qquad (4.20)$$

$$\varphi_a = A_1 \, (e^{x} - e^{p_a x}) \qquad \text{for } x \leq 0 \qquad (4.21)$$

A_1 can be eliminated with boundary condition (7) so that

$$\varphi_P = - A_2 \left[\frac{1 - p_P}{1 - p_a} \left(e^{x} - e^{p_a x} \right) \right] \qquad \text{for } x \leq 0 \qquad (4.22)$$

Similarly for $\beta = 0$

$$\varphi_P = A_8 \, x \, e^{-x} \qquad \text{for } x \geq 0 \qquad (4.23)$$

$$\varphi_a = A_8 \, x \, e^{x} \qquad \text{for } x \leq 0 \qquad (4.24)$$

Combining Equations (4.7), (4.19), (4.20) and (4.22) and introducing

$$\zeta_a = \frac{\partial \sigma_0}{\partial C_a}, \; \zeta_P = \frac{\partial \sigma_0}{\partial C_P} \text{ and } \zeta_t = \frac{\partial \sigma_0}{\partial T}$$

then, for $\beta \neq 0$

$$\left[\zeta_a \frac{\partial C_a}{\partial y} + \zeta_P \frac{\partial C_P}{\partial y} + \zeta_t \frac{\partial T}{\partial y} \right] \Big|_{x=0} =$$

$$= A_2 \, \mu_P \, \alpha^2 \, e^{i\alpha y} \, e^{\beta t} \, (p_P - 1) \left[(1 + p_P) + \frac{\mu_a}{\mu_P} (1 + p_a) + \frac{\alpha \mu_s}{\mu_P} \right] \qquad (4.25)$$

Similarly for $\beta = 0$

$$\left[\zeta_a \frac{\partial C_a}{\partial y} + \zeta_P \frac{\partial C_P}{\partial y} + \zeta_t \frac{\partial T}{\partial y} \right] \Big|_{x=0} = 2 \, A_8 \, \mu_P \, \alpha^2 \, e^{i \, y} \left(1 + \frac{\mu_a}{\mu_P} + \frac{\alpha \, \mu_s}{2 \mu_P} \right) \qquad (4.26)$$

Equation (4.25) describes the evolution with time of a disturbance of wavelength $\lambda = 2\pi/\alpha$ while Equation (4.26) gives the wavenumber of a disturbance that neither grows nor decays with time. This is the state of neutral stability.

In order to obtain α and β from Equations (4.25) and (4.26) the concentration gradients $\frac{\partial C_a}{\partial y}$ and $\frac{\partial C_P}{\partial y}$ have to be found from the equations of diffusion. The temperature gradient $\frac{\partial T}{\partial y}$ has to be obtained from the equation of energy.

In the following sections the temperature gradient $\frac{\partial T}{\partial y}$ is assumed equal to zero and the characteristic equation for an isothermal system is developed. The inclusion of the temperature gradient $\frac{\partial T}{\partial y}$ in the development of the characteristic equation for the case of a system with heat effects is considered in Section 4.6.

4.2.2 Equations of diffusion

The two–dimensional diffusion equation, for a binary mixture of constant mass density is given by

$$\frac{\partial C}{\partial t} + u \frac{\partial C}{\partial x} + v \frac{\partial C}{\partial y} = D \left(\frac{\partial^2 C}{\partial x^2} + \frac{\partial^2 C}{\partial y^2}\right) \qquad (4.27)$$

where u and v are defined in Equations (4.4) and (4.7).

It is assumed that in the undisturbed system constant fluxes have been established and that the undisturbed concentrations are given by

$$C_a^0 = C_a + L_a x \qquad x \geq 0 \qquad (4.28)$$

$$C_P^0 = C_P + L_P x \qquad x \leq 0 \qquad (4.29)$$

The concentration profiles are then disturbed by a perturbation G (x,y,t) caused by the perturbed velocity profiles, so that

$$C = C^0 (x) + G (x,y,t) \tag{4.30}$$

Introducing Equation (4.30) into Equation (4.27) and neglecting second order terms,

$$\frac{\partial G}{\partial t} + u \frac{\partial C^0}{\partial x} = D \left(\frac{\partial^2 G}{\partial x^2} + \frac{\partial^2 G}{\partial y^2}\right) \tag{4.31}$$

The concentration perturbation is of a similar form as the one introduced in the equations of motion, Equation (4.7), i.e.

$$G = H (x) e^{i\alpha y} e^{\beta t} \tag{4.32}$$

Introducing this equation together with Equations (4.4), (4.7), (4.28) and (4.29) into Equation (4.31) an equation for the concentration disturbance, H (x), is obtained:

$$H'' - \left(1 + \frac{\beta}{\alpha^2 D}\right) H = - \frac{i L}{\alpha D} \varphi \tag{4.33}$$

The solution for this equation, for each phase, is given by,

$$H_p = A_9 e^{q_p x} + A_{10} e^{-q_p x} - l_p I_p \tag{4.34}$$

$$H_a = B_9 e^{q_a x} + B_{10} e^{-q_a x} - l_a I_a \tag{4.35}$$

where,

$$I = e^{qx} \int e^{-2qx} \int e^{qx}\, \varphi\, (dx)^2 \qquad (4.36)$$

$$q = \sqrt{1 + \frac{\beta}{\alpha^2 D}} \qquad (4.37)$$

$$l = \frac{i L}{\alpha D} \qquad (4.38)$$

From the boundary conditions for the diffusion equation, constants A_9, A_{10}, B_9 and B_{10} can be calculated. Values of the integrals I_p and I_a may be found in Table 4.1, taken from Sternling and Scriven's work (3).

4.2.2.1 Boundary conditions

The boundary conditions for the diffusion equation are:

(9) and (10) The concentration disturbance vanishes at large distances from the interface:

$$C_p\ (\infty) = C_p^0\ (\infty) \rightarrow H_p\ (\infty) = 0$$

$$C_a\ (-\infty) = C_a^0\ (\infty) \rightarrow H_a\ (-\infty) = 0$$

(11) There is a chemical reaction at the interface, so that the mass balance is given by

$$D_a \left(\frac{\partial C_a}{\partial x}\right) + (k_2\, C_p - k'_1\, C_a) = 0 \qquad \text{at } x=0 \qquad (4.39)$$

where

$$k'_1 = k_1\, C_b$$

(12) Since the stoichiometric factors in the chemical reaction are the same, the fluxes of A and P at the interface are equal, i.e.

$$D_a \left(\frac{\partial C_a}{\partial x}\right) = D_P \left(\frac{\partial C_P}{\partial x}\right) \qquad \text{at } x = 0$$

4.2.2.2 Calculation of H_a and H_P

Expressions for H_a and H_P are found by taking into consideration boundary conditions (9) and (10). Equations (4.34) and (4.35) become:

$$H_P = A_{10}\, e^{-q_P x} - l_P\, I_P \tag{4.40}$$

$$H_a = B_9\, e^{q_a x} - l_a\, I_a \tag{4.41}$$

Introducing the concentration perturbation, defined by Equation (4.32) into Equation (4.30) and using boundary condition (11), in the undisturbed state, the following equation is obtained

$$D_a\, \alpha\, H'_a(0) + [k_2\, H_P(0) - k'_1\, H_a(0)] = 0 \tag{4.42}$$

where, from Equations (4.40) and (4.41),

$$H_P(0) = A_{10} - l_P\, I_P(0) \tag{4.43}$$

$$H_a(0) = B_9 - l_a\, I_a(0) \tag{4.44}$$

$$H'_P(0) = -\, A_{10}\, q_P - l_P\, I'_P(0) \tag{4.45}$$

$$H'_a(0) = B_9\, q_a - l_a\, I'_a(0) \tag{4.46}$$

From boundary condition (12) in the undisturbed state and using Equations (4.30), (4.32), (4.40) and (4.41) the following equation is obtained:

$$D_P\,[-\,A_{10}\,q_P - l_P\,I'_P(0)] = D_a\,[B_9\,q_a - l_a\,I'_a(0)] \qquad (4.47)$$

Constants A_{10} and B_9 may be evaluated from Equations (4.42) and (4.47). Their algebraic values are presented in Output "OUT 1", in Chapter 5.

A_{10} and B_9 may be introduced into Equations (4.43) and (4.44), respectively, and after substitution of the integrals, given in Table 4.1, the expressions for H_a and H_P are found.

4.2.3 Calculation of A and B

To calculate $\frac{\partial C_P}{\partial y}$ and $\frac{\partial C_a}{\partial y}$ to be introduced in Equation (4.25), Equations (4.30) and (4.32) were used so that,

$$\left(\frac{\partial C_P}{\partial y}\right)_{x=0} = \left(\frac{\partial G_P}{\partial y}\right)_{x=0} = H_P(0)\;i\;\alpha\;e^{i\,y}\;e^{\beta t} \qquad (4.48)$$

$$\left(\frac{\partial C_a}{\partial y}\right)_{x=0} = \left(\frac{\partial G_a}{\partial y}\right)_{x=0} = H_a(0)\;i\;\alpha\;e^{i\,y}\;e^{\beta t} \qquad (4.49)$$

Therefore, neglecting heat effects, Equation (4.25) becomes,

$$[\;\zeta_P\,H_P(0)\,i + \zeta_a\,H_a(0)\,i\;]\Big|_{x=0} =$$

$$= A_2\,\mu_P\,\alpha\,(p_P - 1)\left[\;(1 + p_P) + \frac{\mu_a}{\mu_P}(1 + p_a) + \frac{\alpha\mu_s}{\mu_P}\;\right] \qquad (4.50)$$

After substituting $H_P(0)$ and $H_a(0)$ into Equation (4.49) and rearranging terms into dimensionless form, the characteristic equation

$$A = \frac{\mu_P \nu_P}{L_P \zeta_P} \alpha^2 = AC \qquad (4.51)$$

is obtained, where A is the dimensionless wave number and AC is the algebraic value developed, which is given in Output "OUT 2", in Appendix A.

A dimensionless growth constant B, may be defined from the following relationship,

$$\frac{B}{A} = p_P^2 - 1 = (q_a^2 - 1)\, d^2 \qquad (4.52)$$

Another form of the characteristic equation can be found by combining Equations (4.51) and (4.52),

$$B = \frac{\mu_P}{L_P \zeta_P} \beta = BC \qquad (4.53)$$

where BC is also given in Output "OUT 2".

4.2.4 Calculation of A_{NS}

The characteristic equation for $\beta = 0$, the neutral stable condition, is obtained by using Equation (4.26) and a similar manipulation of terms as for $\beta \neq 0$. The final equation is

$$A_{NS} \equiv \frac{\mu_P \nu_P}{L_P \zeta_P} \alpha^2_{NS} = AC_{NS} \qquad (4.54a)$$

where AC_{NS} is presented in Output "OUT 4", in Appendix A, or in dimensionless form:

$$AC_{NS} = \frac{(r^2 - 1)\left[(m + 1)\, r^2 - Z\, (r^2 + 1) \right]}{8\, d^2 \left[(m\, r^2 + 1) - Z \right] \left[1 + \mu_a/\mu_p + \alpha\mu_s/2\mu_p \right]} \qquad (4.54b)$$

This equation was developed by manipulating Equation (4.54a) so that AC_{NS} is presented as a function of the dimensionless terms r^2, m and Z. These dimensionless terms are defined as

$$r^2 = \frac{D_p}{D_a}, \quad m = \frac{k'_1}{k_2} \quad \text{and} \quad Z = \frac{D_p\, \alpha}{k_2}$$

4.3 Analysis of the characteristic equation

The characteristic equation is a function of the physical properties of the system under study as well as the reaction constants of the interfacial chemical reaction involved. For each wave number α, the characteristic equation gives the value of the growth constant β. The wavenumber α is real and positive while β is complex,

$$\beta = \beta_r + \beta_i\, i \qquad (4.55)$$

The system is stable if β_r, the real part of β, is negative for all values of α. If it is positive for only some values of α, the system is still considered unstable.

Table 4.2 shows several types of instabilities which may set in, for different values of β.

For the cases when $\beta_r = 0$, the disturbance neither grows nor decays with time, thus representing the boundary between stable and unstable states. These cases are the neutral stationary and neutral oscillatory regimes

The introduction of ϵ defined in terms of α and β,

$$\epsilon = \frac{\beta}{\alpha^2 D_p} \tag{4.56}$$

simplifies the analysis of the characteristic equation, which may be considered now dependent only on the variable ϵ.

From Equation (4.52)

$$A = \frac{B}{d^2 \epsilon} \tag{4.57}$$

the dimensionless wavenumber A, may be described now as a complex function of the complex variable $\epsilon = \epsilon_r + \epsilon_i\, i$. Therefore, Equation (4.57) may be expressed as,

$$(A_r + A_i\, i)\,(\epsilon^2_r + \epsilon^2_i) = \frac{1}{d^2}\left[B_r\,\epsilon_r + B_i\,\epsilon_i + (B_i\,\epsilon_r - B_r\,\epsilon_i)\, i\right] \tag{4.58}$$

The dimensionless wave number A is real so the imaginary part of A must be zero, and therefore

$$B_i\,\epsilon_r - B_r\,\epsilon_i = 0 \tag{4.59}$$

The ranges of ϵ_r and ϵ_i that satisfy this equation and respective type of instability regime are shown in Table 4.3.

The limiting behaviour of functions A (ϵ) and B (ϵ) is examined in the following sections so that an understanding of the stationary and oscillatory regimes may be obtained.

4.4 Limiting behaviour of the characteristic equation

The development of the limiting behaviour of the characteristic equation, for $\epsilon \to 0$ and $\epsilon \to \infty$ is presented in Appendix B.

When $\epsilon \to 0$, A and B are of the form:

$$A = A_{NS} (1 - f\epsilon) \tag{4.60}$$

$$B = \frac{1}{d^2} A_{NS} (\epsilon - f\epsilon^2) \tag{4.61}$$

where A_{NS} is given by Equation (4.54) and f is in Output "OUT 5" in Appendix A.

When $\epsilon \to \infty$, A and B contain a large number of terms which the computer software used is unable to manipulate analytically. Consequently, only the limiting behaviour of the characteristic equation for very small values of ϵ is analysed in this work.

4.5 Stability analysis

The boundary between stable and unstable states is represented by the neutral stationary and oscillatory regimes. Therefore, these regimes are analysed in detail in the following sections.

4.5.1 Neutral Stationary Regime: $\epsilon_r = 0$ and $\epsilon_i = 0$

When $\epsilon = 0$, Equations (4.60) and (4.61) become

$$A = A_{NS}$$
$$B = 0$$

The conditions for the onset of stationary instabilities are found when the dimensionless wave number for neutral stability A_{NS}, as defined by Equation (4.54) is analysed.

The sign of A_{NS} depends on the signs of ζ_P and L_P, since α^2_{NS} is real and positive. Table 4.4 shows the sign taken by AC_{NS} for the range of values used in this work and assuming that μ_s is equal to zero. For $r^2 > 1$ and $\zeta_P < 0$, A_{NS} has the same sign as AC_{NS} when $L_P < 0$. For $L_P > 0$ they have the same sign when $r^2 < 1$ for $\zeta_P < 0$.

By definition, ϵ is equal to zero either when $\beta = 0$ or when $\alpha = \infty$. The former case was the one analysed previously. From Equation (4.61), when $\alpha = \infty$, B is also zero, so the stationary instability does not grow with time.

When $\epsilon \rightarrow 0$, Table 4.5 shows the sign taken by the factor f for the same range of physical properties investigated before.

The final "sign analysis", for small values of ϵ and when $\zeta_P < 0$, indicates that, for stationary instabilities to occur, mass transfer must be out of phase A into phase P when $r^2 > 1$ and out of phase P into phase A when $r^2 < 1$.

4.5.2 Neutral Oscillatory Regime: $\epsilon_r = 0$ and $\epsilon_i \neq 0$

The neutral oscillatory regime was analysed for small values of ϵ, by considering Equation (4.61) as

$$B = \frac{1}{d^2} A_{NS} (\epsilon_r + \epsilon_i i) - f (\epsilon_r + \epsilon_i i)^2 \qquad (4.62)$$

or for $\epsilon_r = 0$

$$B = \frac{1}{d^2} A_{NS} \epsilon_i i \qquad (4.63)$$

Table 4.6 shows that B takes the same sign as A_{NS}, for different values of r^2. The sign of A_{NS} depends on the signs of ζ_P and L_P, as previously mentioned. For $r^2 > 1$ and $\zeta_P < 0$, B has the same sign as A_{NS} when $L_P < 0$. For $L_P > 0$ they have the same sign when $r^2 < 1$ for $\zeta_P < 0$. Therefore, the system seems to be unstable for the same direction of transfer as in the case of the stationary regime. However, in order to cover all possible unstable conditions the limit of B for $\epsilon \to \infty$ should be analysed. This is impossible with the software facilities available at the moment, as mentioned in Appendix B.

4.6 Energy equation for a system with heat effects

In Section 4.2 a characteristic equation was developed for an isothermal system after neglecting the temperature gradient $\frac{\partial T}{\partial y}$ in the equations of motion. However, the addition of heat effects requires not only the solution of the Navier–Stokes equation and the diffusion equation but

also the energy equation. This equation is given by

$$\frac{\partial T}{\partial t} + u \frac{\partial T}{\partial x} + v \frac{\partial T}{\partial y} = \kappa_t \left(\frac{\partial^2 T}{\partial x^2} + \frac{\partial^2 T}{\partial y^2} \right) \qquad (4.64)$$

The boundary conditions which need to be taken into consideration for the solution of Equation (4.64) are:

(i) the energy balance at the interface is given by

$$Q\ N_j = k_{tp} \left(\frac{\partial T_p}{\partial x}\right) - k_{ta} \left(\frac{\partial T_a}{\partial y}\right) \qquad (4.65)$$

where Q is the heat of reaction, N is the flux and the subscript j can be either a or p depending on the direction of the chemical reaction.

(ii) there is thermal equilibrium at the interface,

$$T_a = T_b \qquad (4.66)$$

The additional inclusion of the energy equation in the development of the characteristic equation for the described system with heat effects introduces such complexity in the theoretical equations that the computer software "REDUCE" was unable to manipulate algebraically the mathematical terms included in the equations. Therefore the final characteristic equation could not be obtained.

4.7 Conclusions

In this chapter the characteristic equation for an isothermal system was developed and analysed. From the stability analysis for the neutral stationary and neutral oscillatory regimes it was concluded that for stationary instabilities to occur mass transfer must be out of the phase with

lower diffusivity. This is the only conclusion that could be drawn analytically. The quantitative effect of the chemical reaction is investigated numerically in Chapter 5.

Oscillatory instabilities as well as the inclusion of heat effects in the the characteristic equation could not be treated due to the limitations of the software "REDUCE". However, the equations have been developed and are ready to be used when more advanced software becomes available.

$\beta \neq 0$	I(0)/a	I'(0)/a
Phase P $x \geq 0$	$\frac{(p^2_P - 1)}{(q^2_P - 1)\ (q^2_P - p^2_P)}$	$\frac{(1 - p_P)\ (q^2_P + p_P)}{(q^2_P - 1)\ (q^2_P - p^2_P)}$
Phase A $x \leq 0$	$-(\frac{1 - p_P}{1 - p_a})\ \frac{(p^2_a - 1)}{(q^2_a - 1)\ (q^2_a - p^2_a)}$	$\frac{(1 - p_P)\ (q^2_a + p_a)}{(q^2_a - 1)\ (q^2_a - p^2_a)}$
$\beta = 0$		
Phase P $x \geq 0$	0	$-1/4$
Phase A $x \leq 0$	0	$-1/4$

TABLE 4.1

Case	β_r	β_i	Type of instability
1	< 0	< 0	stable
2	$= 0$	$= 0$	neutral stationary
3	> 0	$= 0$	stationary
4	$= 0$	> 0	neutral oscillatory
5	> 0	> 0	oscillatory

TABLE 4.2

		Regime
$\epsilon_r = 0$	$\epsilon_i = 0$	neutral stationary
$\epsilon_r \neq 0$	$\epsilon_i = 0$	stationary
$\epsilon_r = 0$	$\epsilon_i \neq 0$	neutral oscillatory
$\epsilon_r \neq 0$	$\epsilon_i \neq 0$	oscillatory

TABLE 4.3

r^2	AC_{NS}	ζ_P	L_P	A_{NS}
> 1	+	−	−	+
< 1	−	−	+	−

TABLE 4.4

Typical data used to establish signs:

$C_B = 10^{-2}$, $D_P = 10^{-9}$, $\mu_s = 0$, $k'_1 = 10^{-12} - 10^{-4}$ and $k_2 = 10^{-10} - 10^{-2}$

r^2	AC_{NS}	$1 - f\ \epsilon_r$	ζ_P	L_P	A
> 1	+	+	−	−	+
< 1	−	+	−	+	−

TABLE 4.5

Typical data used to establish signs:

$C_B = 10^{-2}$, $D_P = 10^{-9}$, $\mu_S = 0$, $k'_1 = 10^{-12} - 10^{-4}$ and $k_2 = 10^{-10} - 10^{-2}$

r^2	A_{NS}	B	ζ_P	L_P
> 1	+	+	−	−
< 1	−	−	−	+

TABLE 4.6

Typical data used to establish signs:

$C_B = 10^{-2}$, $D_P = 10^{-9}$, $\mu_S = 0$, $k'_1 = 10^{-12} - 10^{-4}$ and $k_2 = 10^{-10} - 10^{-2}$

CHAPTER 5

NUMERICAL RESULTS AND DISCUSSION

5.1 Introduction

The characteristic equation developed in Chapter 4 was used to study numerically the stability of four liquid–liquid systems with interfacial chemical reactions. In this chapter results of that study are presented for the case of stationary instabilities and a comparison is made with similar results obtained from computations performed using Sternling and Scriven's characteristic equation for diffusional mass transfer.

The simulation of the systems was classified into four cases depending on the value of the diffusivity ratio, r^2:

Case 1 — $r^2 = 4.0$

Case 2 — $r^2 = 1.5$

Case 3 — $r^2 = 1.0$

Case 4 — $r^2 = 0.5$

For each case two values of the viscosity ratio e^2 were used: $e^2 = 0.5$ and $e^2 = 2.0$.

The above data and selected values of the physical properties are representative of typical liquid–liquid systems.

The characteristic equation, Equation (4.51), was developed assuming a pseudo–first order interfacial chemical reaction of the form

$$A + B \underset{\leftarrow}{\overset{\rightarrow}{}} P$$

with a flux given by

$$N_a = k'_1 C_a - k_2 C_p$$

where: $k'_1 = k_1 C_b$; k_1 and k_2 are the forward and the reverse reaction rate constants respectively; and C_a, C_b and C_p are the concentrations of compounds A, B and P respectively.

The pseudo–forward reaction rate constant k'_1 and the reverse reaction rate constant k_2 were varied so that the effect of the rate of reaction could be investigated.

The choice of the range of numerical values chosen for the interfacial reaction rate constants was guided by experimental values reported in the literature (71) (72).

Results presented here were obtained assuming that the variation of interfacial tension with concentration, ζ, is negative; that the composite surface viscosity, μ_s, is negligible and that the concentration of the extractant, C_b, is in excess. Numerical values used throughout this work are:

$$\zeta_p = -1 \times 10^{-4} \text{ m}^3/\text{s}^2$$

$$\mu_s = 0$$

$$C_b = 1 \times 10^{-2} \text{ kg/m}^3$$

5.2 Numerical calculation of α_{NS}, α and β

Figure 5.1 shows the flowchart used in the calculation of α_{NS}, the neutral stability wavenumber. From an initial guess, α_{NS} was iterated until the numerical values of each side of Equation (4.54a) were the same. The sign taken by the parameter L_p, which determines the direction of transfer, is also defined to obey that equality. Taking into consideration the definition of wavelength as $\lambda = 2\pi/\alpha$, wavenumbers which may lead to

instabilities must be below the calculated value of α_{NS}, which corresponds to the minimum wavelength for the onset of instabilities.

Figure 5.2 presents the flowchart for the calculation of the growth constant β, for different values of wavenumber α below α_{NS}. For each value of α, a correct value of β is obtained when, after an initial guess of β, the equality given by Equation (4.51) is satisfied.

5.3 Discussion of results

The physical behaviour of the systems studied is expressed and discussed in terms of the relationship between the wavenumber α and the growth constant β.

For each case results are presented in a table which is divided in two parts: the first gives computed values using Sternling and Scriven's diffusion model and the second computed values using the interfacial reaction model. The latter table contains results for different values of the pseudo–forward and reverse reaction rate constants, k'_1 and k_2. Values for the physical properties used to obtain these numerical results are included prior to the tables.

Figures 5.3, 5.4, 5.6, 5.7 show plots of α vs β for the interfacial reaction model for all the cases found unstable. Each curve has a maximum which corresponds to the wavenumber which is amplified most rapidly and eventually dominates the system, i.e. α_D. The maximum value of α, which is α_{NS}, occurs when $\beta = 0$. Below this value instabilities grow with time.

It may also be observed that instabilities with small wavelengths have large growth constants and instabilities with large wavelength have small growth constants: large instability cells grow more slowly due to the larger

inertia of the greater amount of fluid which has to be displaced for the instability to grow.

The graphs in Figures 5.3, 5.4 and 5.6 also show that the values of α and β obtained from the computations of Sternling and Scriven's model are smaller than the ones computed using the interfacial reaction model. Therefore a system is more unstable when a chemical reaction occurs at the interface.

It is important to emphasize that this study is only concerned with stationary instabilities, so that when a system is referred to as being stable or unstable it is meant to be in terms of stationary instabilities only.

5.3.1 Effect of diffusivity ratio r^2 and viscosity ratio e^2

Table 5.1 shows the effect of the diffusivity ratio in the unstable direction of mass transfer, L_p, for a negative system. When L_p is negative mass transfer occurs from phase A into phase P (forward reaction); when it is positive the reverse reaction is taking place and leads to the opposite direction of transfer.

An analysis of the results shown in Table 5.1 confirms that the systems studied are unstable for either the forward or the reverse reactions depending on whether r^2 is greater or less than 1. Thus the onset of stationary instabilities occurs when mass transfer is out of the phase of lower diffusivity. In each case the system is stable in the opposite direction from the one shown in the table.

Results given in Tables 5.2 and 5.3 and in Figures 5.3, 5.4 and 5.5 suggest that for the conditions used, values of α and β increase with increasing values of r^2. This may be seen in Figure 5.5 for Cases 1 and 2.

The unstable direction corresponds to the direction of the forward reaction and for the same values of D_P, k'_1 and k_2 the system is more unstable when the ratio of diffusivities is larger, i.e. the value of D_a is lower. Since simulations have been conducted at constant interfacial flux, a decrease in the value of D_a results in a steeper concentration gradient for reactant A, thus making the system more unstable.

An analysis of Tables 5.2 – 5.5 also shows that the viscosity ratio e^2 does not affect the values of α and β.

According to Sternling and Scriven's work the value of the ratio of the viscosities becomes important when oscillatory instabilities are considered and they have concluded that for a negative system oscillatory instabilities occur when mass transfer is out of the phase of higher viscosity.

When $r^2 = 1$ both diffusivities are exactly the same and the characteristic equation for neutral stability becomes zero. In Case 3a and Case 3b values of $r^2 = 1.0001$ and $r^2 = 0.9999$ were used to investigate the sensitivity of the system in a region close to $r^2 = 1$. Results obtained, which may be seen in Table 5.1, show that a small variation on the value of the diffusivity ratio produces stationary instabilities in opposite directions of mass transfer. Therefore, it is important to emphasize that since diffusivities are usually estimated from correlations or measured with experimental errors larger than the accuracy required by this model, the stability of a system in which $r^2 \cong 1$ is difficult to predict.

The sensitivity of the interfacial reaction model in the region of $r^2 \cong 1$, may explain the disagreement between predictions using the Sternling and Scriven's model and experimental results reported by Thompson and Perez de Ortiz (28). They observed instabilities in the extraction

of uranyl–nitrate from an aqueous solution to an organic phase containing tri–n–butylphosphate and mention that there is chemical reaction at the interface.

They measured the interfacial tension of this system and found that it increases with increasing concentrations ($\zeta > 0$); they estimated that the diffusivity ratio was approximately unity and the viscosity ratio was approximately two. According to Sternling and Scriven's stability criteria this system should exhibit oscillatory instabilities. When the organic phase was replaced with hexane, so that the viscosity ratio modified to $e^2 = 0.6$, instabilities were still visible. If these instabilities were purely oscillatory, according to Sternling and Scriven's criteria they should disappear when $e^2 < 1$. However, since this system seems to have a value of $r^2 \cong 1$, from the conclusions mentioned previously it may still present stationary instabilities which are independent of the value of the viscosity ratio.

5.3.2 Effect of k_1 and k_2

The onset of stationary instabilities in systems with an interfacial reaction of the type presented in this work, has been analysed for different values of the forward and the reverse reaction rate constants, k_1 and k_2 respectively.

As previously mentioned, the value of the wavenumber of neutral stability, i.e. α_{NS}, suggests how unstable a system is. The calculation of α_{NS} is performed, as described in Section 4.2, using Equation (4.54a). In this section Equation (4.54b) is used to discuss the effect of k'_1 and k_2 on the values of α_{NS}. Equation (4.54b) was developed by manipulating the terms in Equation (4.54a) so that AC_{NS} is presented as a function of the

dimensionless terms r^2, m and Z. These dimensionless terms have been defined as

$$r^2 = \frac{D_p}{D_a}$$

$$m = \frac{k'_1}{k_2}$$

and

$$Z = \frac{D_p \alpha}{k_2}$$

Changes to any of these dimensionless terms may therefore affect the final value of α_{NS}.

The effect on r^2, m and Z of changes in the parameters which define them is summarized in Table 5.7.

It is important to point out that Z is also a function of α. However, in the discussion presented here the effect of α on the value of Z is not considered.

In Cases 1, 2, 3 and 4, all physical properties were kept constant and although variations in the pseudo forward reaction rate constant k'_1 are discussed, they correspond to changes in the forward reaction constant k_1, with the value of C_b kept constant.

Table 5.1 shows that in Cases 1 and 2 the unstable direction of mass transfer is when the net flux is from Phase A to Phase P. In Case 4, instabilities occur when the net flow is from Phase P to Phase A. In order that Cases 1, 2 and 4 can be discussed and compared easily, for the same direction of net flux, a system which mirrors Case 4 has been defined: Case 4 (rev). This case was simulated numerically by adjusting all

parameters in such a way that properties of Phase A and Phase P in Case 4 became properties of Phase P and Phase A in Case 4 (rev). Having introduced the changes, Case 4 (rev) is unstable in the direction of the forward reaction. Numerical data used for Case 4 (rev) are shown in Table 5.6.

5.3.2.1 Case 1, Case 2, Case 4 and Case 4 (rev)

The effect of k'_1 and k_2 on Cases 1 and 2 is presented in Tables 5.1b and 5.2b These tables show that a change in the value of k'_1, with k_2 constant, does not affect the values of either α or β. However, a decrease in the value of k_2, for the same value of k'_1, produces an increase in the values of α and β. This effect may be seen in Plots (1) and (2) in Figures 5.3 and 5.4. Therefore in Cases 1 and 2 the size of the instabilities is a function of k_2 but remains unaffected by a variation in k'_1.

Results for Case 4 and Case 4 (rev) are shown in Tables 5.5 and 5.6 and plotted in Figures 5.6 and 5.7.

As previously mentioned, Case 4 (rev) is the one which is to be discussed. An analysis of the results for this case indicates that the values of α and β are functions of k'_1 and not of k_2.

Table 5.8 presents a summary of the effect of k'_1 and k_2 on α_{NS} for Cases 1, 2, 4 and 4 (rev).

It is important to notice that the most relevant difference between Case 2 and Case 4 (rev), is that although values of r^2 are not very different, the value of D_P in Case 4 (rev) is double. This increase in the value of D_P affects the values of AC_{NS} in Equation (4.54b). According to Table 5.7, when all the other parameters are kept constant, an increase in

D_P produces an increase in Z and hence a variation in AC_{NS}. This variation is also dependent on m, when k'_1 is varied. The relative magnitude of the terms m and Z will determine the value of α_{NS}. When D_P increases, a variation in k_2 will only affect the individual values of m and Z but not their value relative to each other. The relative magnitude of m and Z is therefore only dependent on k'_1.

To understand the reason for the shift of the dependence of α_{NS} on k_2, in Case 2, to k'_1 in Case 4 (rev), a qualitative analysis of the mechanism of instabilities is necessary.

The rate of dissipation of an interfacial excess concentration of A depends on: the net rate of interfacial reaction, the rate of diffusion of A back to Phase A and the rate of diffusion of the product P into Phase P. Since the value of r^2 in this discussion is always greater than unity, it is assumed that the diffusion of A does not contribute significantly to the dissipation of A from the interface. The process can then be controlled by k'_1, k_2 and D_P. In the lower range of values of D_P considered, as in Cases 1 and 2, the excess of P produced by the forward reaction remains at the interfacial region long enough for the reverse reaction to take part in the rate controlling process. Thus, the higher the value of k_2, the less steep the interfacial concentration gradient of C_{ai} and the more stable the system. This is represented in Table 5.8 and in Figure 5.5. As D_P increases, the rate of diffusional dissipation of P increases until a point is reached when the reverse reaction ceases to influence the process. At this stage the interfacial gradient of A becomes a function of k'_1.

5.3.3 Comparison with the diffusional stability model

5.3.3.1 Cases 1, 2 and 3

Data used in Case 1 and Case 2 was also used to compute results using Sternling and Scriven's diffusion model. Results are presented in Tables 5.2a and 5.3a and plotted in Plot (3) of Figures 5.3 and 5.4. From these it may be seen that a system with an interfacial reaction, of the type assumed in this work, is more unstable than a system where interfacial mass transfer is by diffusion only.

Figures 5.3 and 5.4 seem to indicate that Sternling and Scriven's model, for the data used in this work, may be close to the case of a system with an interfacial chemical reaction when $k_2 \cong \infty$ (very fast reverse reaction). At constant interfacial concentration and for a constant net flux, any increase in k_2 is accompanied by an increase in k'_1. Hence, both forward and reverse reactions become faster and equilibrium at the interface is approached. The system would then become controlled by diffusional transfer, i.e. the Sternling and Scriven's model.

In Case 3, values of the wavenumber and the growth constant are very small. Therefore the only values presented in Table 5.4, for the interfacial chemical reaction model and for Sternling and Scriven's model, are for the neutral stability case. The system is very close to stability which would be the case if $r^2 = 1$, as the characteristic equation would become equal to zero.

It may also be observed in Table 5.4 that although α_{NS} is higher for the case of the interfacial reaction model, i.e. the system is more unstable than in Sternling and Scriven's case, the values of α_{NS} are still very small: instabilities are of very large wavelength.

5.4 Summary of results

It may be concluded from the results discussed in this chapter that the onset of stationary instabilities for a system with a reversible pseudo first–order interfacial chemical reaction is not only dependent on r^2, but also in two additional dimensionless terms, i.e. m and Z. The stability analysis is very complex and general criteria could not be established. However, numerical results have been explained qualitatively and the following conclusions may be drawn:

(1) instabilities occur for both directions of mass transfer;

(2) the value of r^2 controls the direction of the instabilities which is the same as for diffusional mass transfer: out of the phase of lower diffusivity;

(3) the interfacial reaction model predicts smaller cells which amplify more quickly (system more unstable) than those predicted by the diffusion model;

(4) stationary instabilities are independent of the ratio of viscosities e^2;

(5) the influence of m and Z is reflected by the effect of k'_1 and k_2 on λ_{NS};

(6) and under certain circumstances, α_{NS} is a function of k'_1 and others of k_2, depending on the potential rate of diffusion in each phase.

Case	r^2	L_p
1	4.0	−
2	1.5	−
3a	1.0001	−
3b	0.9999	+
4	0.5	+

TABLE 5.1

CASE 1

$L_p = L_a/r^2 = -1.0 \times 10^5$ kg/m^4

$D_p = 2.0 \times 10^{-9}$ m^2/s

$\nu_p = 1.0 \times 10^{-6}$ m^2/s

$\mu_s = 0$

$\mu_p = 1.0 \times 10^{-3}$ Kg/ms

$\mu_a/\mu_p = 0.5$

$r^2 = 4.0$

$e^2 = 2.0$ or 0.5

$\alpha \times 10^{-5}$	β
9.97	0
8.0	170
3.0	320
1.0	170
0.0	0

TABLE 5.2a

Diffusion model

$\frac{k'_1}{1.1}$	$\frac{k_2}{6.6}$	$\alpha \times 10^{-5}$	β
10^{-12}	10^{-10}	25	0
		16	1500
		10	2000
		4	1500
		0	0
10^{-12}	10^{-2}	22	0
		16	900
		10	1400
		4	900
		0	0
10^{-4}	10^{-10}	25	0
		16	1500
		10	2000
		4	1500
		0	0
10^{-4}	10^{-2}	22	0
		16	900
		10	1400
		4	900
		0	0

TABLE 5.2b

Interfacial reaction model

CASE 2

$L_P = L_a/r^2 = -1.0 \times 10^5$ kg/m^4

$D_P = 2.0 \times 10^{-9}$ m^2/s

$\nu_P = 1.0 \times 10^{-6}$ m^2/s

$\mu_s = 0$

$\mu_P = 1.0 \times 10^{-3}$ Kg/ms

$\mu_a/\mu_P = 0.5$

$r^2 = 1.5$

$e^2 = 2.0$ or 0.5

$\alpha \times 10^{-5}$	β
3.5	0
2.5	96
1.6	105
1.0	85
0.5	65
0.0	0

TABLE 5.3a

Diffusion model

$\frac{k'_1}{1.1}$	$\frac{k_2}{6.6}$	$\alpha \times 10^{-5}$	β
10^{-12}	10^{-10}	7.2	0
		5.0	240
		3.5	350
		2.0	280
		0	0
10^{-12}	10^{-2}	5.5	0
		4.0	120
		3.0	175
		1.0	100
		0	0
10^{-4}	10^{-10}	7.2	0
		5.0	240
		3.5	350
		2.0	280
		0	0
10^{-4}	10^{-2}	5.5	0
		4.0	120
		3.0	175
		1.0	100
		0	0

TABLE 5.3b

Interfacial reaction model

CASE 3

$L_p = L_a/r^2 = \pm 1.0 \times 10^5$ kg/m^4

$D_p = 2.0 \times 10^{-9}$ m^2/s

$\nu_p = 1.0 \times 10^{-6}$ m^2/s

$\mu_s = 0$

$\mu_p = 1.0 \times 10^{-3}$ Kg/ms

$\mu_a/\mu_p = 0.5$

$r^2 = 1.0001$ ($L_p < 0$) or 0.9999 ($L_p > 0$)

$e^2 = 2.0$ or 0.5

	$\alpha_{NS} \times 10^{-3}$	β	$\frac{k'_1}{1.1}$	$\frac{k_2}{6.6}$
Diffusion model	4.5	0	–	–
Interfacial reaction model	9.1	0	10^{-12}	10^{-10}
	6.8	0	10^{-12}	10^{-2}

TABLE 5.4

CASE 4

$L_p = L_a/r^2 = + 1.0 \times 10^5$ kg/m^4

$D_p = 2.0 \times 10^{-9}$ m^2/s

$\nu_p = 1.0 \times 10^{-6}$ m^2/s

$\mu_s = 0$

$\mu_p = 1.0 \times 10^{-3}$ Kg/ms

$\mu_a/\mu_p = 0.5$

$r^2 = 0.5$

$e^2 = 2.0$ or 0.5

$\alpha \times 10^{-5}$	β
2.6	0
2.0	50
1.19	71
0.5	50
0.0	0

TABLE 5.5a

Diffusion model

$\frac{k'_1}{1.1}$	$\frac{k_2}{6.6}$	$\alpha \times 10^{-5}$	β
10^{-12}	10^{-10}	5.6	0
		3.0	300
		2.0	330
		1.0	240
		0.0	0
10^{-12}	10^{-2}	3.3	0
		2.0	100
		1.5	120
		0.5	67
		0.0	0
10^{-4}	10^{-10}	5.6	0
		3.0	300
		2.0	330
		1.0	240
		0.0	0
10^{-4}	10^{-2}	3.3	0
		2.0	100
		1.5	120
		0.5	67
		0	0

TABLE 5.5b

Interfacial reaction model

CASE 4 (rev)

$L_p = L_a/r^2 = -0.5 \times 10^5$ kg/m^4

$D_p = 4.0 \times 10^{-9}$ m^2/s

$\nu_p = 0.5 \times 10^{-6}$ m^2/s

$r^2 = 2.0$

$\mu_s = 0$

$\mu_p = 0.5 \times 10^{-3}$ Kg/ms

$\mu_a/\mu_p = 2.0$

$e^2 = 2.0$ or 0.5

$\frac{k'_1}{1.1}$	$\frac{k_2}{6.6}$	$\alpha \times 10^{-5}$	β
10^{-10}	10^{-12}	5.6	0
		3.0	300
		2.0	330
		1.0	240
		0.0	0
10^{-2}	10^{-12}	3.3	0
		2.0	100
		1.5	120
		0.5	67
		0.0	0

TABLE 5.6

(continues next page)

(cont'd)

10^{-10}	10^{-4}	5.6	0
		3.0	300
		2.0	330
		1.0	240
		0.0	0
10^{-2}	10^{-4}	3.3	0
		2.0	100
		1.5	120
		0.5	67
		0	0

TABLE 5.6

Interfacial reaction model

Parameter changed	Terms affected
D_P	r^2 and Z
D_a	r^2
k'_1	m
k_2	m and Z

TABLE 5.7

Case	$L_p \times 10^{-5}$	$D_p \times 10^9$	$D_a \times 10^9$	r^2	$\frac{k_1}{1.1}$	$\frac{k'_1}{1.1}$	$\frac{k2}{6.6}$	$\alpha_{NS} \times 10^{-5}$	Comments
1	−1.0	2.0	0.5	4.0	10^{-10}	10^{-12}	10^{-10}	25.0	$f(k_2)$
					10^{-10}	10^{-12}	10^{-2}	22.0	
					10^{-2}	10^{-4}	10^{-10}	25.0	
					10^{-2}	10^{-4}	10^{-10}	22.0	
2	−1.0	2.0	1.3	1.5	10^{-10}	10^{-12}	10^{-10}	7.2	$f(k_2)$
					10^{-10}	10^{-12}	10^{-2}	5.5	
					10^{-2}	10^{-4}	10^{-10}	7.2	
					10^{-2}	10^{-4}	10^{-2}	5.5	
4 (rev)	−0.5	4.0	2.0	2.0	10^{-8}	10^{-10}	10^{-12}	5.6	$f(k'_1)$
					10^{-8}	10^{-10}	10^{-4}	5.6	
					10^{0}	10^{-2}	10^{-12}	3.3	
					10^{0}	10^{-2}	10^{-4}	3.3	
4	+1.0	2.0	4.0	0.5	10^{-10}	10^{-12}	10^{-10}	5.6	$f(k_2)$
					10^{-10}	10^{-12}	10^{-2}	3.3	
					10^{-2}	10^{-4}	10^{-10}	5.6	
					10^{-2}	10^{-4}	10^{-2}	3.3	

TABLE 5.8

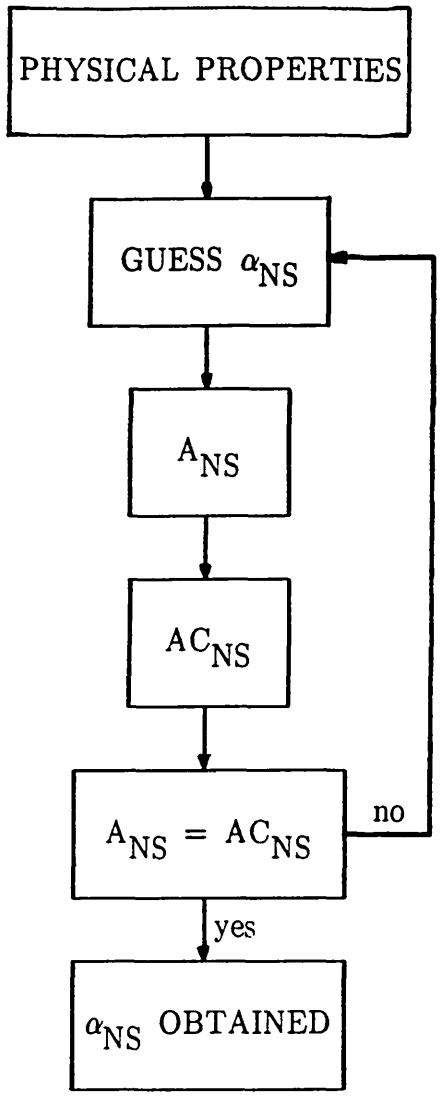

FIGURE 5.1

Flowchart for the calculation of α_{NS}

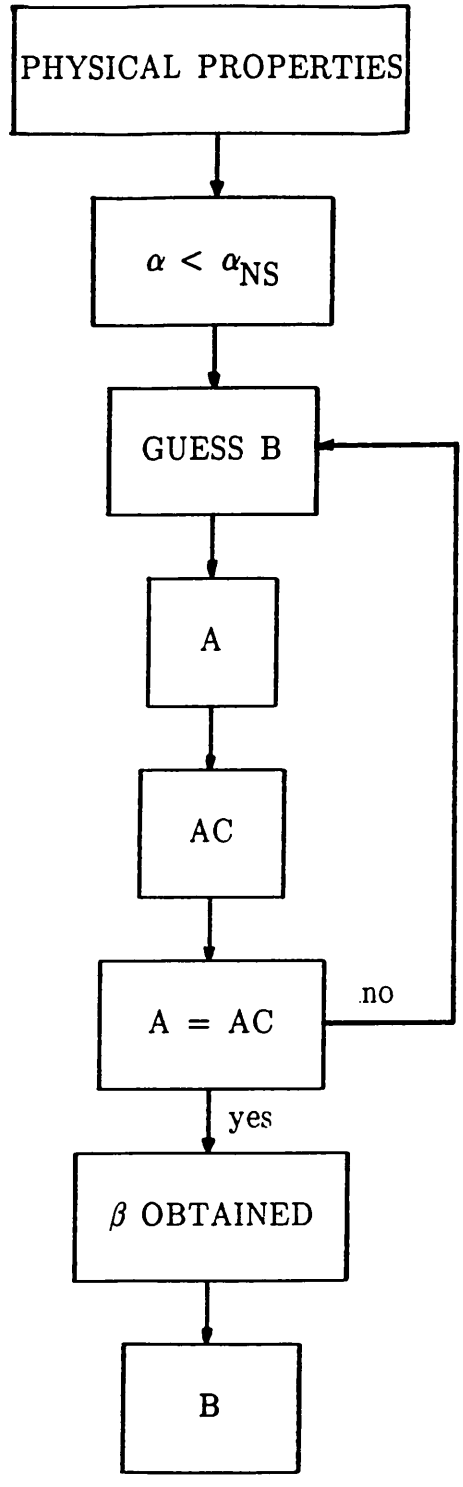

FIGURE 5.2

Flowchart for the calculation of β for each α

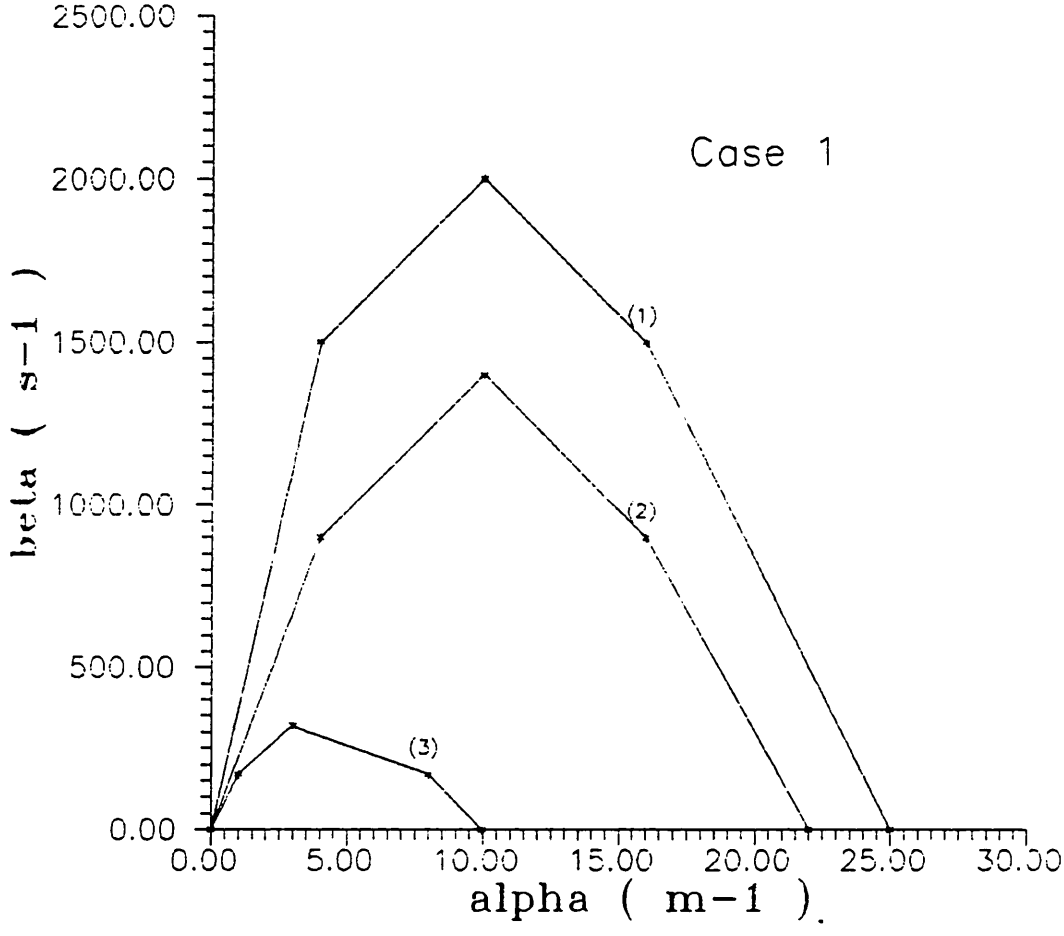

FIGURE 5.3

$r^2 = 4.0$; $k'_1 = 1.1\times10^{-4}$ and $k'_1 = 1.1\times10^{-12}$

(1) $k_2 = 6.6\times10^{-10}$

(2) $k_2 = 6.6\times10^{-2}$

(3) Sternling and Scriven's model

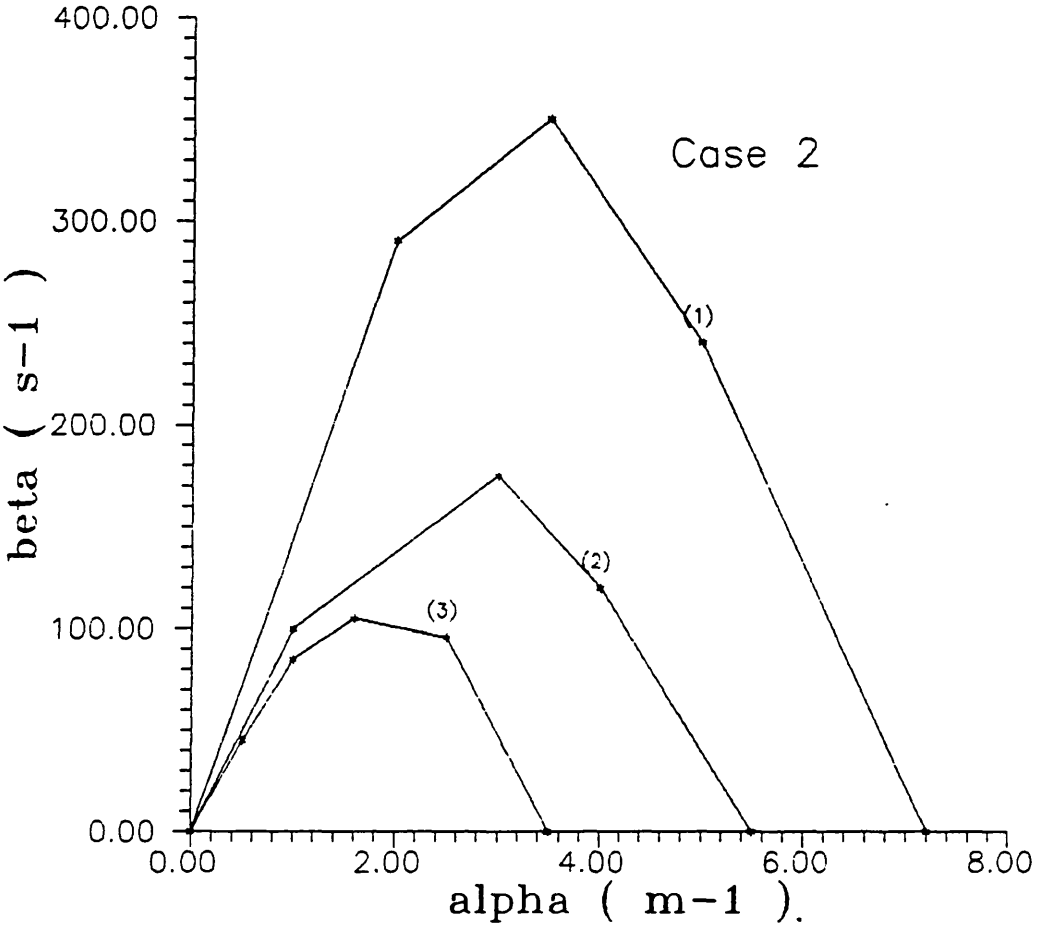

FIGURE 5.4

$r^2 = 1.5$; $k'_1 = 1.1\times10^{-4}$ and $k'_1 = 1.1\times10^{-12}$

(1) $k_2 = 6.6\times10^{-10}$

(2) $k_2 = 6.6\times10^{-2}$

(3) Sternling and Scriven's model

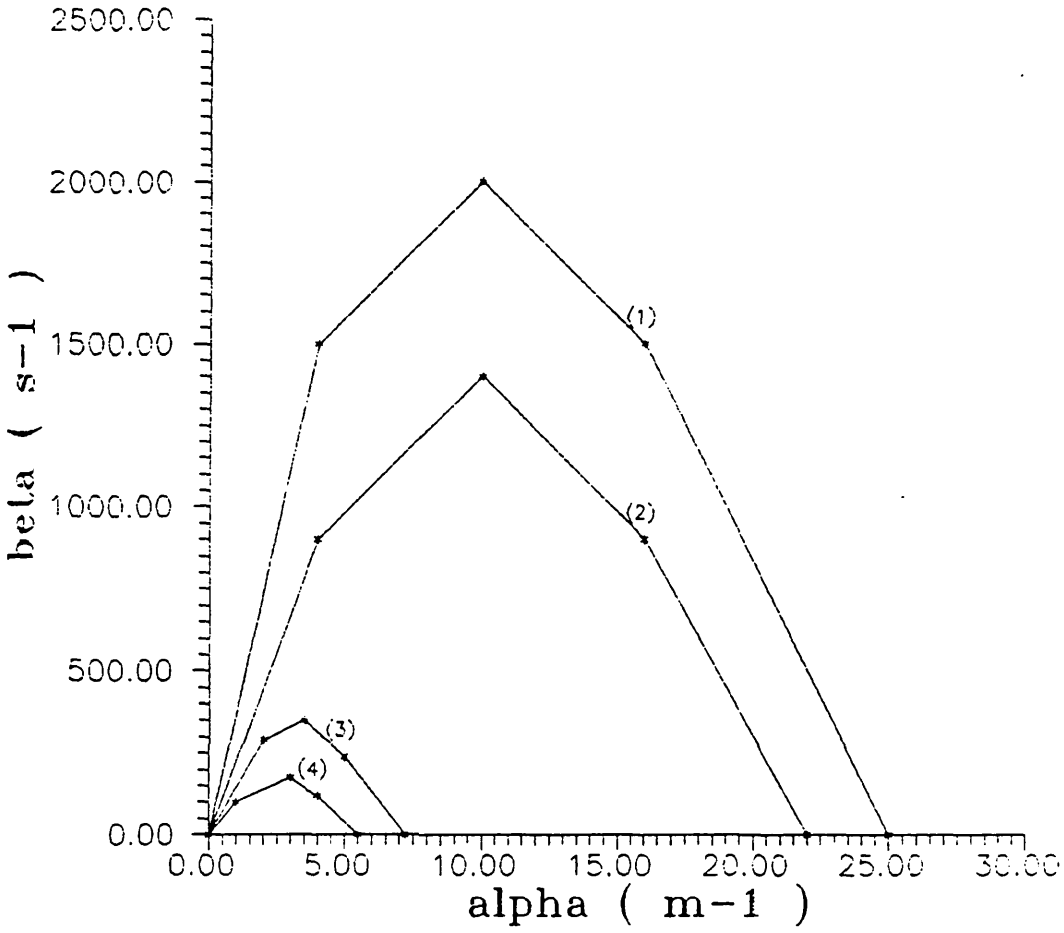

FIGURE 5.5

(1) $r^2 = 4.0$; $k'_1 = 1.1\times10^{-12}$ and $k_2 = 6.6\times10^{-10}$

(2) $r^2 = 4.0$; $k'_1 = 1.1\times10^{-12}$ and $k_2 = 6.6\times10^{-2}$

(3) $r^2 = 1.5$; $k'_1 = 1.1\times10^{-12}$ and $k_2 = 6.6\times10^{-10}$

(4) $r^2 = 1.5$; $k'_1 = 1.1\times10^{-12}$ and $k_2 = 6.6\times10^{-2}$

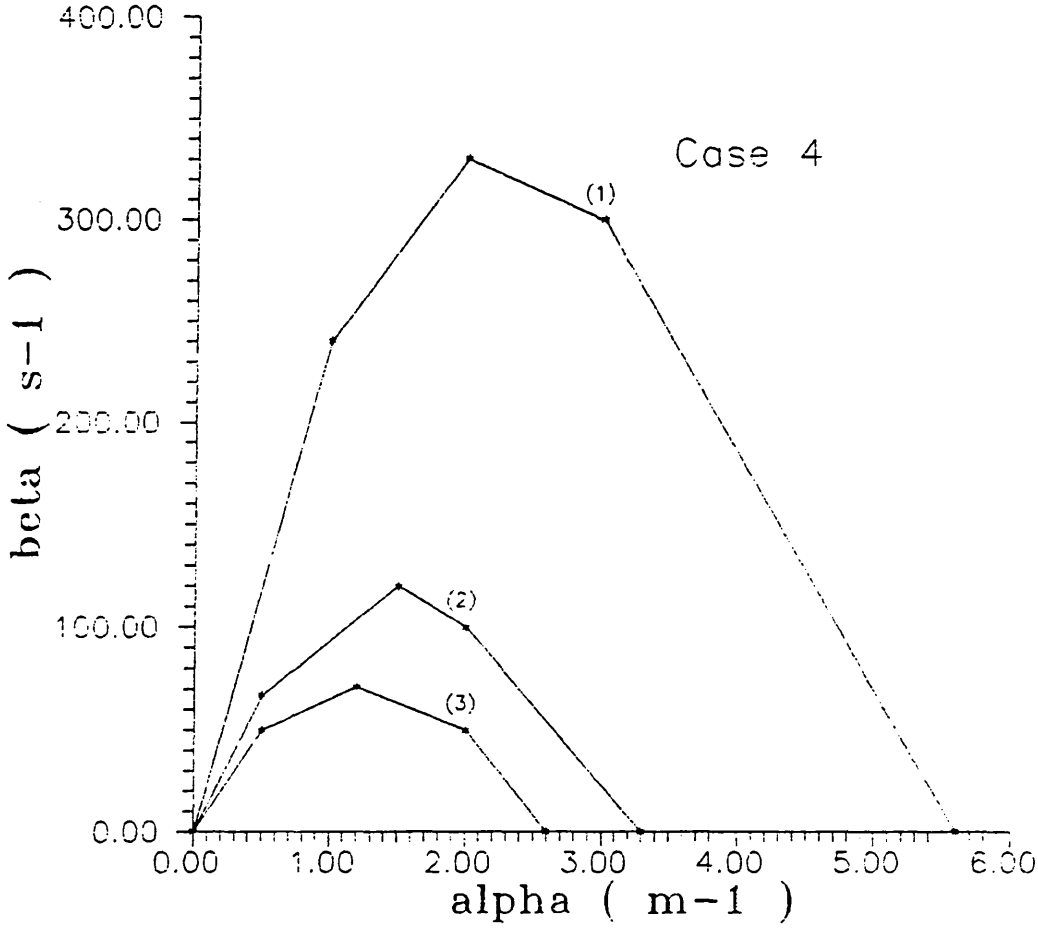

FIGURE 5.6

$r^2 = 0.5$; $k'_1 = 1.1\times10^{-4}$ and $k'_1 = 1.1\times10^{-12}$

(1) $k_2 = 6.6\times10^{-10}$

(2) $k_2 = 6.6\times10^{-2}$

(3) Sternling and Scriven's model

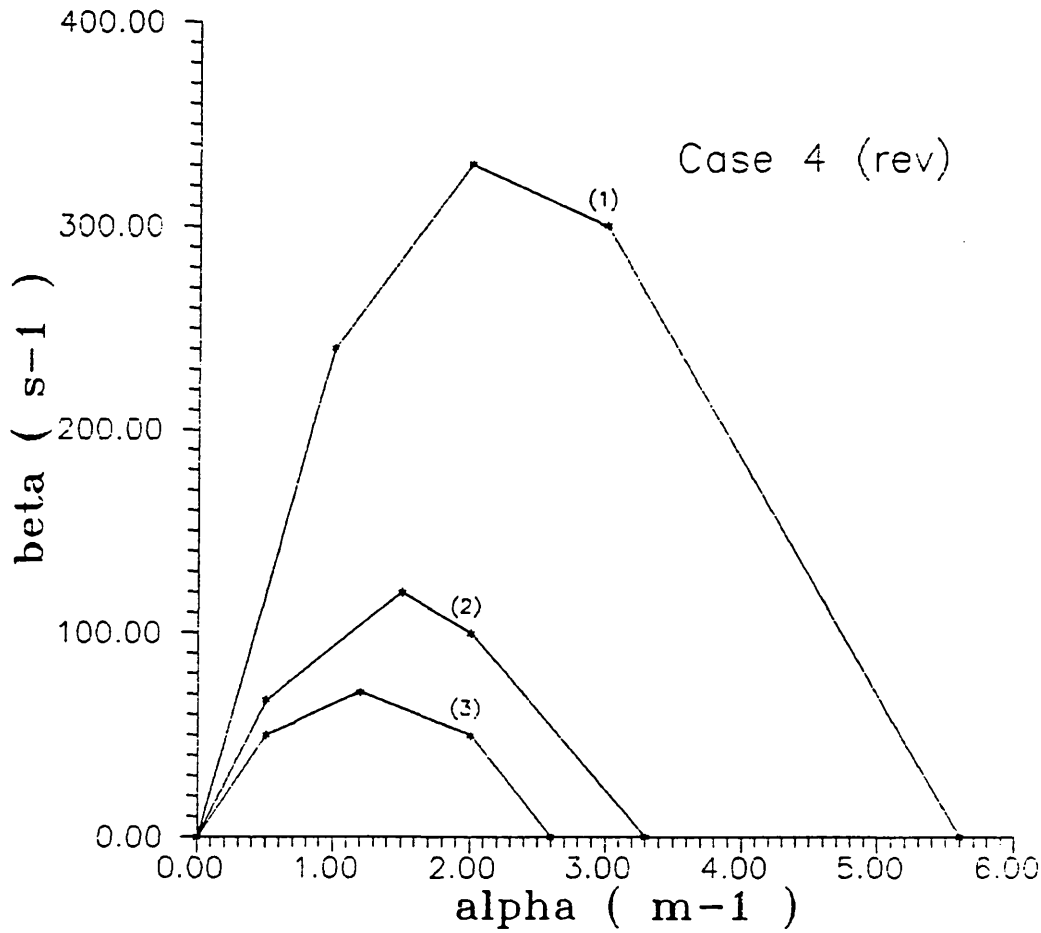

FIGURE 5.7

$r^2 = 2.0$; $k_2 = 6.6\times10^{-4}$ and $k_2 = 6.6\times10^{-12}$

(1) $k'_1 = 1.1\times10^{-10}$

(2) $k'_1 = 1.1\times10^{-2}$

(3) Sternling and Scriven's model

CHAPTER 6

CONCLUSIONS

The conclusions taken from this work may be summarized as follows:

(1) Under microgravity conditions, temperature gradients were sufficient to initiate Marangoni instabilities, although those initiated were of shorter duration than instabilities under gravitational conditions.

(2) The analysis of the characteristic equation, for a system with a pseudo first–order reversible chemical reaction and for small values of ϵ, indicates that stationary instabilities occur when mass transfer is out of the phase of lower diffusivity, for negative systems. This agrees with the stability criteria established by Sternling and Scriven for a liquid–liquid system with diffusional mass transfer.

(3) For the unstable direction of mass transfer and for the range of values used, when the diffusivity ratio increases the system presents instabilities of smaller size and larger amplification factor.

(4) Stationary instabilities are independent of the ratio of viscosities.

(5) A system with an interfacial pseudo first–order reversible chemical reaction is more unstable than a system with mass transfer by diffusion only.

(6) The size of the instabilities is a function of the forward reaction constant or of the reverse reaction constant, depending on the potential rate of diffusion in each phase.

RECOMMENDATIONS FOR FURTHER WORK

(1) The heat of solution for the system ethylacetoacetate/water should be calculated so that clear conclusions can be taken from the microgravity experiments performed in this work.

(2) Similar experiments to the ones executed under microgravity should be performed with different binary systems and with liquid–liquid systems with an interfacial chemical reaction. This would enable a more complete study of the thermal effects on the onset of Marangoni instabilities.

(3) If gravitational effects are found to be important in liquid–liquid systems with an interfacial reaction the model presented in this work should be modified to take these effects into account.

(4) More advanced software capabilities should be found so that:

   (i) stability criteria for the system under the conditions investigated could be established;

   (ii) a similar analysis to the one in the present work could be performed for oscillatory instabilities;

   (iii) and the present interfacial reaction model could be extended by the addition of heat effects.

APPENDIX A

COMPUTER LISTINGS AND OUTPUTS

A.1 Algebraic solution

The development of mathematical equations for the determination of the characteristic equation Equation (4.51) and of the equations needed for its analysis, was achieved using one of the University of London Computer Centre computers: the AMDAHL 5890. The algebraic programing system "REDUCE", was used to deal with very long, tedious calculations. The disc operating system control language used in the programs to access "REDUCE" was "PHOENIX 3".

Listings of the computer programs written and respective outputs are included in this Appendix.

The nomenclature used throughout this work, could not always be the same as in the computer programs. All variables are defined in the list of symbols included at the end of this thesis.

```
setuplocal (out=.out1/w/1b)
reduce %1!
comment      FILE 1
comment      CALCULATION OF A10 AND B9 FOR BETA ≠ 0;
off nat;
factor h,m,alfa;
off exp;
on gcd;
dia:=((1-pp)*(qa**2+pa))/((qa**2-1)*(qa**2-pa**2));
dip:=((1-pp)*(qp**2+pp))/((qp**2-1)*(qp**2-pp**2));
ia:=(-((1-pp)*(pa**2-1))/((1-pa)*(qa**2-1)*(qa**2-pa**2)));
ip:=(pp**2-1)/((qp**2-1)*(qp**2-pp**2));
dha:=b9*qa-la*dia;
hp:=a10-lp*ip;
ha:=b9-la*ia;
eq1:=da*alfa*dha+h*(hp-m*ha);
eq2:=dp*(-a10*qp-lp*dip)-da*(b9*qa-la*dia);
solve(lst(eq1,eq2),lst(a10,b9));

out out;
write "output out 1";
a10:=soln(1,1);
b9:=soln(1,2);
write";end";
on nat;
quit;
!
```

```
output out 1$

A10 := ( - (H*M*PA*QA*PP*DP*LP + H*M*PA*QA*DP*LP*QP**2 + H*M*PA*PP*
DP*LP + H*M*PA*DP*LP*QP**2 + H*M*QA**2*PP*DP*LP + H*M*
QA**2*DP*LP*QP**2 + H*M*QA*PP*DP*LP + H*M*QA*DP*LP*QP**
2 + H*M*PP**2*DA*LA*QP**2 - H*M*PP**2*DA*LA - H*M*DA*LA
*QP**4 + H*M*DA*LA*QP**2 + H*PA*QA**2*PP*DA*LP + H*PA*
QA**2*DA*LP + H*PA*QA*PP*DA*LP + H*PA*QA*DA*LP + H*QA**
3*PP*DA*LP + H*QA**3*DA*LP + H*QA**2*PP*DA*LP + H*QA**2
*DA*LP - PA*QA**2*PP*ALFA*DP*DA*LP - PA*QA**2*ALFA*DP*
DA*LP*QP**2 - PA*QA*PP*ALFA*DP*DA*LP - PA*QA*ALFA*DP*DA
*LP*QP**2 - QA**3*PP*ALFA*DP*DA*LP - QA**3*ALFA*DP*DA*
LP*QP**2 - QA**2*PP*ALFA*DP*DA*LP - QA**2*ALFA*DP*DA*LP
*QP**2)*(PP - 1))/((H*M*DP*QP + H*QA*DA - QA*ALFA*DP*DA
*QP)*(PA + QA)*(QA + 1)*(PP**2 - QP**2)*(QP**2 - 1))$

B9 := ((H*M*PA*PP*DP*LA*QP**2 + H*M*PA*PP*DP*LA*QP + H*M*PA*DP*LA*
QP**3 + H*M*PA*DP*LA*QP**2 + H*M*PP*DP*LA*QP**2 + H*M*PP*DP
*LA*QP + H*M*DP*LA*QP**3 + H*M*DP*LA*QP**2 + H*PA**2*QA**2*
DP*LP - H*PA**2*DP*LP + H*PA*PP*DA*LA*QP + H*PA*PP*DA*LA +
H*PA*DA*LA*QP**2 + H*PA*DA*LA*QP - H*QA**4*DP*LP + H*QA**2*
PP*DA*LA*QP + H*QA**2*PP*DA*LA + H*QA**2*DP*LP + H*QA**2*DA
*LA*QP**2 + H*QA**2*DA*LA*QP - PA*PP*ALFA*DP*DA*LA*QP**2 -
PA*PP*ALFA*DP*DA*LA*QP - PA*ALFA*DP*DA*LA*QP**3 - PA*ALFA*
DP*DA*LA*QP**2 - QA**2*PP*ALFA*DP*DA*LA*QP**2 - QA**2*PP*
ALFA*DP*DA*LA*QP - QA**2*ALFA*DP*DA*LA*QP**3 - QA**2*ALFA*
DP*DA*LA*QP**2)*(PP - 1))/((H*M*DP*QP + H*QA*DA - QA*ALFA*
DP*DA*QP)*(PA**2 - QA**2)*(QA**2 - 1)*(PP + QP)*(QP + 1))$

;end$
```

```
 setuplocal (in=.out1/r/fb)
 setuplocal (out=.out2/w/fb)
reduce %i!
comment      FILE 2
comment      CALCULATION OF AC AND BC FOR BETA ≠ 0;
off echo;
off nat;
in in;
on gcd;
off factor;
off exp;
 ia:=(-((1-pp)*(pa**2-1))/((1-pa)*(qa**2-1)*(qa**2-pa**2)));
 ip:=(pp**2-1)/((qp**2-1)*(qp**2-pp**2));
  tt3:=(pp-1)*(1+pp+nia*(1+pa)/nip+alfa*nis/nip);
eq33:=ic*sa*(b9-la*ia)+ic*sp*(a10-lp*ip);
eq3:=eq33/tt3;

qp**2:=qp1;
qa**2:=qa1;
pp**2:=pp1;
pa**2:=pa1;
ic**2:=ic1;
sub(qp1=1+ep,qa1=1+(ep*dp/da),pp1=1+(ep*dp/niup),pa1=1+(ep*niup/niua
*dp/niup),lp=ic*llp/(alfa*dp),la=ic*lla/(alfa*da),eq3);
eq5:=ws;
 sub(ic1=-1,ep=beta/(alfa**2*dp),eq5);
 eq6:=ws;
out out;
 write "output out2 ";
ac:=eq6*niup*alfa/(sp*llp);
bc:=eq6*beta/(sp*llp*alfa);
write";end";
on nat;
quit;
!
```

```
output out2 $

AC := ((((((PP + 1)*QP*LLA - (PA + 1)*QA*LLP - PA*LLP)*ALFA**2*DA
 - (BETA + ALFA**2*DA)*LLP)*DP + (DP*ALFA**2 + BETA)*LLA*
DA + DP*PP*LLA*ALFA**2*DA)*(M*SP + SA)*H - ((PP + 1) + QP)
*(DP*ALFA**2 + BETA)*DP*LLA*SA*ALFA*DA + ((PA*ALFA**2*DA +
BETA + ALFA**2*DA)*QA + (PA + 1)*(BETA + ALFA**2*DA))
*DP*LLP*SP*ALFA*DA - QP*DP**2*PP*LLA*SA*ALFA**3*DA)*NIUP*
NIP)/(((M*QP*DP + QA*DA)*H - QP*DP*QA*ALFA*DA)*((PP + 1)*NIP
 + (PA + 1)*NIA + NIS*ALFA)*(QP + PP)*(QP + 1)*(QA
 + PA)*(QA + 1)*DP*LLP*SP*ALFA**2*DA)$

BC := ((((((PP + 1)*QP*LLA - (PA + 1)*QA*LLP - PA*LLP)*ALFA**2*DA
 - (BETA + ALFA**2*DA)*LLP)*DP + (DP*ALFA**2 + BETA)*LLA*
DA + DP*PP*LLA*ALFA**2*DA)*(M*SP + SA)*H - ((PP + 1) + QP)
*(DP*ALFA**2 + BETA)*DP*LLA*SA*ALFA*DA + ((PA*ALFA**2*DA +
BETA + ALFA**2*DA)*QA + (PA + 1)*(BETA + ALFA**2*DA))
*DP*LLP*SP*ALFA*DA - QP*DP**2*PP*LLA*SA*ALFA**3*DA)*BETA*
NIP)/(((M*QP*DP + QA*DA)*H - QP*DP*QA*ALFA*DA)*((PP + 1)*NIP
 + (PA + 1)*NIA + NIS*ALFA)*(QP + PP)*(QP + 1)*(QA
 + PA)*(QA + 1)*DP*LLP*SP*ALFA**4*DA)$

;end$
```

```
setuplocal (out=.out3/w/fb)
reduce %i!
comment      FILE 3
comment      CALCULATION OF A1Ø AND B9 FOR BETA = Ø;
off nat;
factor h,m,alfa;
off exp;
on gcd;
ia:=Ø;
ip:=Ø;
dia:=-1/4;
dip:=-1/4;
ga:=1;
gp:=1;
dha:=b9*ga-la*dia;
hp:=a1Ø-lp*ip;
ha:=b9-la*ia;
la:=ic*lla/(alfa*da);
lp:=ic*llp/(alfa*dp);
eq1:=da*alfa*dha+h*(hp-m*ha);
eq2:=dp*(-a1Ø*gp-lp*dip)-da*(b9*ga-la*dia);
solve(lst(eq1,eq2),lst(a1Ø,b9));

out out;
write "output out3";
a1Ø:=soln(1,1);
b9:=soln(1,2);
write";end";
on nat;
quit;
;
```

```
OUTPUT OUT 3$

A1Ø := (((LLP - LLA)*H*M - ALFA*LLP*DA)*IC)/(4*ALFA*((M*DP + DA)*h
  - ALFA*DP*DA))$

B9 := (((LLP - LLA)*H + ALFA*DP*LLA)*IC)/(4*ALFA*((M*DP + DA)*H -
ALFA*DP*DA))$

;end$
```

```
setuplocal (in=.out3/r)
 setuplocal (out=.out4/w/fb)
reduce %i!
comment      FILE 4
comment      CALCULATION OF ACNS;
off echo;
off nat;
in in;
on factor;
on gcd;
off exp;
ia:=0;
ip:=0;
ic**2:=-1;
eq33:=ic*sa*(b9-la*ia)+ic*sp*(a10-lp*ip);
 tt3:=2*(1+nia/nip+(alfa*nis)/(2*nip));
eq3:=eq33/tt3;

out out;
 write "output out 4";
acns:=ws*niup*alfa/(sp*llp);
write";end";
on nat;
quit;
!
```

```
output out 4$

ACNS := ((((LLA - LLP)*H*M + DA*ALFA*LLP)*SP + ((LLA - LLP)*H - DP*
ALFA*LLA)*SA)*NIUP*NIP)/(4*((M*DI + DA)*H - DP*DA*ALFA
)*(ALFA*NIS + 2*NIP + 2*NIA)*LLP*SP)$

;end$
```

```
 setuplocal (in=.out1/r/fb)
 setuplocal (out=.out5/w/fb)
reduce %i!
comment      FILE 5
comment      CALCULATION OF THE LIMITS OF A AND FACTOR F
comment      FOR SMALL VALUES OF EP;
off echo;
off nat;
in in;
on gcd;
on factor;
off exp;
 ia:=(-((1-pp)*(pa**2-1))/((1-pa)*(ga**2-1)*(ga**2-pa**2)));
 ip:=(pp**2-1)/((gp**2-1)*(gp**2-pp**2));
  tt3:=(pp-1)*(1+pp+nia*(1+pa)/nip+alfa*nis/nip);
eg33:=ic*sa*(b9-la*ia)+ic*sp*(a10-lp*ip);
eg3:=eg33/tt3;

gp**2:=gp1;
ga**2:=ga1;
pp**2:=pp1;
pa**2:=pa1;
ic**2:=ic1;
sub(gp1=1+ep,ga1=1+(ep*dp/da),pp1=1+(ep*dp/niup),pa1=1+(ep*niup/nia
*dp/niup),lp=ic*llp/(alfa*dp),la=ic*lia/(alfa*da),eg3);
eg5:=ws;
 comment sub(ic1=1,ep=beta/(alfa**2*dp),eg5);
sub(ic1=-1,eg5);
 eg6:=ws;
 r2:=dp/da;
e2:=niup/niua;
d2:=dp/niup;
 gp:=sqrt(1+ep);
ga:=sqrt(1+(r2*ep/2));
pp:=sqrt(1+(d2*ep/2));
pa:=sqrt(1+(e2*d2*ep/2));
a:=eg6*niup*alfa/(sp*llp);
on exp;
 let ep**2=0;
factor ep;
numa:=num(a);
dena:=den(a);
n2:=lterm(numa,ep);
d2:=lterm(dena,ep);
n1:=numa-n2;
d1:=dena-d2;
iden:=(1/d1)*(1-d2/d1);
proa:=numa*iden;
sub(ep=0,proa);
proa0:=ws;
on factor;
off exp;
 f1:=1-proa/ans;
f2:=(d2/d1)-(n2/n1);
out out;
comment write "output out 5 ";
factor ep;
lima:=proa;
ans:=proa0;
f:=f2/ep;
write";end";
on nat;
quit;
!
```

```
output out 5 $

LIMA := (((((((((4*SP + 3*SA)*EP - 4*SA)*(NIS*ALFA + 2*NIP + 2*NIA)
*NIUP + 2*EP*SP*NIP*DA)*NIUA + (NIS*ALFA + 2*NIP + 4
*NIA)*NIUP*EP*SP*DA)*LLA - 2*((NIS*ALFA + 4*NIP +
2*NIA)*NIUA + 2*NIUP*NIA)*LLP*EP*SP*DA)*DP*DA +
(2*((NIS*ALFA + 2*NIP + 2*NIA)*NIUP + NIP*DA)*NIUA + (
NIS*ALFA + 2*NIP + 4*NIA)*NIUP*DA)*DP**2*LLA*EP*SA
 + (5*LLA*EP - 4*LLA - 16*LLP*EP + 8*LLP)*(NIS*ALFA + 2
*NIP + 2*NIA)*NIUA*NIUP*SP*DA**2)*M*DP - (((4*(2*EP
 - 1)*(NIS*ALFA + 2*NIP + 2*NIA)*NIUP*SA + (
NIS*ALFA + 4*NIP + 2*NIA)*EP*SP*DA)*NIUA + 2
*NIUP*EP*SP*NIA*DA)*LLP - 4*(EP - 2)*(NIS*ALFA + 2
*NIP + 2*NIA)*LLA*NIUA*NIUP*SA)*DP*DA**2 - (((((NIS
*ALFA + 4*NIP + 2*NIA)*DA + 2*(NIS*ALFA + 2*
NIP + 2*NIA)*NIUP)*NIUA + 2*NIUP*NIA*DA)*LLP
 - 2*(2*(2*(NIS*ALFA + 2*NIP + 2*NIA)*NIUP + NIP*DA)*
NIUA + (NIS*ALFA + 2*NIP + 4*NIA)*NIUP*DA)*LLA)*DP
**2*EP*SA*DA - 4*(EP - 1)*(NIS*ALFA + 2*NIP + 2*NIA)*LLP
*NIUA*NIUP*SP*DA**3)*M*ALFA + (((NIS*ALFA + 4*NIP + 2*
NIA)*NIUA + 2*NIUP*NIA)*LLP*EP*SP*DA - (3*EP - 4
)*(NIS*ALFA + 2*NIP + 2*NIA)*LLA*NIUA*NIUP*SA)*DP**
2*ALFA**2*DA**2 - (2*(2*(NIS*ALFA + 2*NIP + 2*NIA)*NIUP
 + NIP*DA)*NIUA + (NIS*ALFA + 2*NIP + 4*NIA)*NIUP*
DA)*DP**3*LLA*EP*SA*ALFA**2*DA - (2*M*DP**2*LLA*NIUA*
NIUP*EP*NIS*ALFA + 4*M*DP**2*LLA*NIUA*NIUP*EP*NIP + 4*
M*DP**2*LLA*NIUA*NIUP*EP*NIA + 2*M*DP**2*LLA*NIUA*EP*
NIP*DA + M*DP**2*LLA*NIUP*EP*NIS*ALFA*DA + 2*M*DP**2*
LLA*NIUP*EP*NIP*DA + 4*M*DP**2*LLA*NIUP*EP*NIA*DA - M*
DP**2*LLP*NIUA*EP*NIS*ALFA*DA - 4*M*DP**2*LLP*NIUA*EP*
NIP*DA - 2*M*DP**2*LLP*NIUA*EP*NIA*DA - 2*M*DP**2*LLP*
NIUP*EP*NIA*DA + 5*M*DP*LLA*NIUA*NIUP*EP*NIS*ALFA*DA
 + 10*M*DP*LLA*NIUA*NIUP*EP*NIP*DA + 10*M*DP*LLA*NIUA*
NIUP*EP*NIA*DA - 4*M*DP*LLA*NIUA*NIUP*NIS*ALFA*DA - 8*
M*DP*LLA*NIUA*NIUP*NIP*DA - 8*M*DP*LLA*NIUA*NIUP*NIA*
DA - 8*M*DP*LLP*NIUA*NIUP*EP*NIS*ALFA*DA - 16*M*DP*LLP
*NIUA*NIUP*EP*NIP*DA - 16*M*DP*LLP*NIUA*NIUP*EP*NIA*DA
 + 4*M*DP*LLP*NIUA*NIUP*NIS*ALFA*DA + 8*M*DP*LLP*NIUA*
NIUP*NIP*DA + 8*M*DP*LLP*NIUA*NIUP*NIA*DA + 4*DP*LLA*
NIUA*NIUP*EP*NIS*ALFA*DA + 8*DP*LLA*NIUA*NIUP*EP*NIP*
DA + 8*DP*LLA*NIUA*NIUP*EP*NIA*DA + 2*DP*LLA*NIUA*EP*
NIP*DA**2 + DP*LLA*NIUP*EP*NIS*ALFA*DA**2 + 2*DP*LLA*
NIUP*EP*NIP*DA**2 + 4*DP*LLA*NIUP*EP*NIA*DA**2 - 2*DP*
LLP*NIUA*NIUP*EP*NIS*ALFA*DA - 4*DP*LLP*NIUA*NIUP*EP*
NIP*DA - 4*DP*LLP*NIUA*NIUP*EP*NIA*DA - DP*LLP*NIUA*EP
*NIS*ALFA*DA**2 - 4*DP*LLP*NIUA*EP*NIP*DA**2 - 2*DP*
LLP*NIUA*EP*NIA*DA**2 - 2*DP*LLP*NIUP*EP*NIA*DA**2 +
LLA*NIUA*NIUP*EP*NIS*ALFA*DA**2 + 2*LLA*NIUA*NIUP*EP*
NIP*DA**2 + 2*LLA*NIUA*NIUP*EP*NIA*DA**2 - 4*LLA*NIUA*
NIUP*NIS*ALFA*DA**2 - 8*LLA*NIUA*NIUP*NIP*DA**2 - 8*
LLA*NIUA*NIUP*NIA*DA**2 - 4*LLP*NIUA*NIUP*EP*NIS*ALFA*
DA**2 - 8*LLP*NIUA*NIUP*EP*NIP*DA**2 - 8*LLP*NIUA*NIUP
*EP*NIA*DA**2 + 4*LLP*NIUA*NIUP*NIS*ALFA*DA**2 + 8*LLP
*NIUA*NIUP*NIP*DA**2 + 8*LLP*NIUA*NIUP*NIA*DA**2)*(M*
SP + SA)*H**2 + 4*(2*EP - 1)*(NIS*ALFA + 2*NIP + 2*NIA
)*DP*LLP*NIUA*NIUP*SP*ALFA**2*DA**3)*NIP)/(16*(H*M*DP
 + H*DA - DP*ALFA*DA)**2*(NIS*ALFA + 2*NIP + 2*NIA)**2*LLP*
NIUA*SP*DA)$


ANS := (((M*SP + SA)*(LLA - LLP)*H - DP*LLA*SA*ALFA + LLP*SP*ALFA*
DA)*NIUP*NIP)/(4*((M*DP + DA)*H - DP*ALFA*DA)*(NIS*ALFA +
2*NIP + 2*NIA)*LLP*SP)$


F := (((((((NIS*ALFA + 4*NIP + 2*NIA)*DA + 2*(NIS*ALFA + 2*NIP + 2*
NIA)*NIUP)*NIUA + (NIS*ALFA + 2*NIP + 4*NIA)*NIUP*DA)
*DP + 8*(NIS*ALFA + 2*NIP + 2*NIA)*NIUA*NIUP*DA)*M*DP + ((
(NIS*ALFA + 4*NIP + 2*NIA)*DA + 4*(NIS*ALFA + 2*NIP
 + 2*NIA)*NIUP)*NIUA + (NIS*ALFA + 2*NIP + 4*NIA)*
NIUP*DA)*DP*DA + 4*(NIS*ALFA + 2*NIP + 2*NIA)*NIUA*NIUP*
DA**2)*H - (((NIS*ALFA + 4*NIP + 2*NIA)*DA + 4*(NIS*ALFA +
2*NIP + 2*NIA)*NIUP)*NIUA + (NIS*ALFA + 2*NIP + 4*
NIA)*NIUP*DA)*DP**2*ALFA*DA - 8*(NIS*ALFA + 2*NIP + 2*
NIA)*DP*NIUA*NIUP*ALFA*LA**2)*((M*SP + SA)*(LLA - LLP)*H
 - DP*LLA*SA*ALFA + LLP*SP*ALFA*DA) + ((((2*NIUA + DA)*LLP
*NIUP - LLA*NIUA*DA)*DP - 3*LLA*NIUA*NIUP*DA)*(M*SP
 + SA)*H - ((4*NIUA + DA)*LLP*SP - 5*LLA*NIUA*SA)*DP*
NIUP*ALFA*LA + DP**2*LLA*NIUA*SA*ALFA*DA)*((M*DP + DA)*H
 - DP*ALFA*DA)*(NIS*ALFA + 2*NIP + 2*NIA))/(4*((M*DP + DA)
*H - DP*ALFA*LA)*((M*SP + SA)*(LLA - LLP)*H - DP*LLA*SA*ALFA
 + LLP*SP*ALFA*DA)*(NIS*ALFA + 2*NIP + 2*NIA)*NIUA*NIUP*DA)$

;end;
```

APPENDIX B

LIMITING BEHAVIOUR OF THE CHARACTERISTIC EQUATION

B.1 Small values of ϵ

The radicals in the characteristic equation, Equation (4.51), have the form $\sqrt{1 + x}$, which can be expanded in binomial series as:

$$(1 - x)^n = 1 + nx + n\,(n - 1)\,\frac{x^2}{2!} + \ldots \qquad \text{(B.1)}$$

This series converges for $x \leq 1$ when $n > 0$ and neglecting terms of second and higher order, expansions of p and q are:

$$p_P = 1 + d^2\,\frac{\epsilon}{2} \qquad p_a = 1 + e^2\,d^2\,\frac{\epsilon}{2} \qquad \text{(B.2)}$$

$$q_P = 1 + \frac{\epsilon}{2} \qquad q_a = 1 + r^2\,\frac{\epsilon}{2} \qquad \text{(B.3)}$$

The numerator and denominator of Equation (4.51), after inserting Equations (B.2) and (B.3) become of the form:

$$\text{NUMA} = N_1 + N_2\,\epsilon + N_3\,\epsilon^2 \qquad \text{(B.5)}$$

$$\text{DENA} = D_1 + D_2\,\epsilon + D_3\,\epsilon^2 + \ldots + D_8\,\epsilon^7 \qquad \text{(B.6)}$$

The inverse of Equation (B.6) may be expanded for small values of ϵ:

$$\frac{1}{\text{DENA}} = \frac{1}{D_1}\left[\,1 - \frac{1}{D_1}\,(\,D_2\,\epsilon + D_3\,\epsilon^2\,)\,\right] \qquad \text{(B.7)}$$

Multiplying Equation (B.6) by Equation (B.7) and neglecting terms of second and higher order:

$$\text{NUMA} \times \frac{1}{\text{DENA}} = \frac{N_1}{D_1}\left[\, 1 - \left(\frac{D_2}{D_1} - \frac{N_2}{N_1} \right) \epsilon \,\right] \qquad \text{(B.8)}$$

or

$$\text{LIMA} = \frac{\text{NUMA}}{\text{DENA}} = AC_{NS}\,(1 - f\,\epsilon) \qquad \text{(B.9)}$$

where AC_{NS} is given by Equation (4.54) and

$$f = \frac{D_2}{D_1} - \frac{N_2}{N_1} \qquad \text{(B.10)}$$

Equations (B.5) to (B.10) are fully expanded in Output "OUT 5" in Chapter 5.

B.2 Large values of ϵ

For large values of ϵ the radicals in the characteristic equation can be rearranged as:

$$p_P = d\sqrt{\epsilon}\sqrt{1 + \frac{1}{d^2\epsilon}} \qquad \text{(B.11)}$$

$$p_a = e\,d\sqrt{\epsilon}\sqrt{1 + \frac{1}{d^2e^2\epsilon}} \qquad \text{(B.12)}$$

$$q_P = \sqrt{\epsilon}\sqrt{1 + \frac{1}{\epsilon}} \qquad \text{(B.13)}$$

$$q_a = r\sqrt{\epsilon}\sqrt{1 + \frac{1}{r^2\epsilon}} \qquad \text{(B.14)}$$

and their expansions, after neglecting terms of higher order than one, are:

$$p_P = d\sqrt{\epsilon}\left[1 + \frac{1}{2d^2\epsilon}\right] \tag{B.15}$$

$$p_a = e\,d\sqrt{\epsilon}\left[1 + \frac{1}{2e^2d^2\epsilon}\right] \tag{B.16}$$

$$q_P = \sqrt{\epsilon}\left[1 + \frac{1}{2\epsilon}\right] \tag{B.17}$$

$$q_a = r\sqrt{\epsilon}\left[1 + \frac{1}{2r^2\epsilon}\right] \tag{B.18}$$

A similar manipulation of terms as previously described for small values of ϵ, was performed for the determination of the limits of A and B when $\epsilon \to \infty$. Unfortunately, the number of terms involved is so large that the final algebraic values are impossible to obtain with the means available for use.

LIST OF SYMBOLS

The nomenclature of the computer programs is presented here in bold and capital letters or normal if it is the same as in the main text.

$A = (\nu_P \ \mu_P/\zeta_P \ L_P) \ \alpha^2$, dimensionless wave number

AC = dimensionless wave number given by Equation (4.51)

A_n = constant of integration

$B = (\nu_P/\zeta_P \ L_P) \ \beta$, dimensionless growth constant

BC = dimensionless growth constant given by Equation (4.53)

B_n = constant of integration

C = concentration, Kmole m^{-3}

D = diffusivity, $m^2 \ s^{-1}$

$d = \sqrt{D_P/\nu_P}$, dimensionless

DEN = denominator

DHA = H'_a

DHP = H'_P

DIA = I'_a

DIP = I'_P

$e = \sqrt{\nu_P/\nu_a}$, dimensionless

f = function defined in Equation (4.60), dimensionless

f( ) = function of the variable in brackets

G = concentration perturbation, Kg m^{-3}

H = X part of the concentration perturbation, Kg m^{-3}

IC = $i = \sqrt{-1}$

k_1 = forward rate of reaction constant, $Kmole^{-1}\ m^3\ s^{-1}$

k'_1 = pseudo–forward rate of reaction constant, s^{-1}

k_2 = reverse rate of reaction constant, s^{-1}

LL = L = undisturbed concentration gradient, $Kg\ m^{-4}$

L = l = $(i/\alpha\ D)\ L$, $Kg\ m^{-5}\ s$

$m = (k_1/k_2)\ C_B$, dimensionless

NUM = numerator

$p = \sqrt{1 + (\beta/\alpha^2\nu)}$, dimensionless

P = pressure, $Kg\ m^{-1}\ s^{-2}$

$q = \sqrt{1 + (\beta/\alpha^2 D)}$, dimensionless

$r = \sqrt{D_p/D_a}$, dimensionless

t = time coordinate, s

U,V,W = X,Y and Z components of velocity, ms^{-1}

X,Y,Z = spatial coordinates, m

$Z = \frac{D_p\ \alpha}{k_2}$, dimensionless

Greek letters

α = **ALFA** = wave number, m^{-1}

β = **BETA** = growth constant, s^{-1}

β_r = amplification factor for the disturbance

β_i = circular frequency

ζ = S = concentration coefficient of interfacial tension, m^3s^{-2}

κ = dilational surface viscosity, ms^{-1}

$\lambda = 2\pi/\alpha$ = wavelength, m

μ = **NI** = ordinary viscosity, $Kg\ m^{-1}s^{-1}$

μ_s = NIS = $\Gamma + \kappa$, composite surface viscosity, Kg s^{-1}

ν = NIU = kinematic viscosity, m^2s^{-1}

ϵ = EP = $\beta/\alpha^2 D_p$,dimensionless

ρ = density, Kg m^{-3}

τ_0 = equilibrium interfacial tension, Kg s

τ_{xy} = y component of the fluid shear stress, Kg $m^{-1}s^{-2}$

τ_{yy} = y component of the longitudinal surface stress, Kg s^{-2}

φ = x part of the stream function, m^2s^{-1}

ψ = stream function, m^2s^{-1}

Γ = surface shear viscosity, m s^{-1}

Subscripts

a = phase A ($x < 0$)

D = dominant unstable disturbance

i = imaginary part of a complex variable

N = neutrally stable disturbance

p = phase P ($x > 0$)

r = real part of a complex variable

S = stationary disturbance

Superscripts

0 = value in the undisturbed state

primes = differentiation sign

LIST OF REFERENCES

(1) Thomson, J., *Philosophical Magazine*, 10, 330 (1855).

(2) Marangoni, C., *Annalen der Physik und Chemie Band* CXLIII, 7 (1871).

(3) Sternling, C. V. and Scriven, L. E., *Journal of the American Institution of Chemical Engineers*, 5, 514 (1959).

(4) Scriven, L.E. and Sternling, C. V., *Nature*, 187, 186 (1960).

(5) Sawistowski, H., *Interfacial phenomena* in *Recent advances in liquid–liquid extraction* (ed. C. Hanson), Pergamon Press, Oxford (1971).

(6) Berg, J.C., In R*ecent developments in separation science*, vol II, C.R.C. Press, Cleveland, Ohio (1972).

(7) Cho, S.H. and Jones, M.A., paper presented at the *21st Canadian Chemical Enginering Conference*, Montreal (1971).

(8) Ortiz, E.S.P. de, and Sawistowski H., *Chemical Engineering Science*, 30, 1527 (1975).

(9) Pearson, J.R.A., *Journal of Fluid Mechanics*, 4, 489 (1958).

(10) Ward, A.F.H. and Brooks, L.H., *Transactions of Faraday Society*, 48, 1124 (1952).

(11) Merson, R.L. and Quinn, J.A., *Journal of the American Institute of Chemical Engineers*, 10, 804 (1964).

(12) Austin, L.J., Ying, W.E. and Sawistowski H., *Chemical Engineering Science*, 21, 1109 (1966).

(13) Ying, W.E. and Sawistowski, H., *Proceedings of the International Solvent Extraction Conference, Society of Chemical Industry*, pp 840 (1971).

(14) Davies, G. A. and Thornton, J.D., *Letters in Heat and Mass Transfer*, 4, 287 (1977).

(15) Ortiz, E.S.P. de, and Sawistowski, H., *Chemical Engineering Science*, 28, 2051 (1973).

(16) Ortiz, E.S.P. de, and Sawistowski, H., *Chemical Engineering Science*, 28, 2063 (1973).

(17) Hancock, T.A., White, J.L. and Spruiell, J.E., *Polymer Engineering and Science*, 20, 1126 (1980).

(18) Aguirre, F.J., Klinzing G.E., Chiang, S.H., Leaf G.K. and Minkoff, M., *Chemical Engineering Science*, 40, 1449 (1985).

(19) Thornton, J.D., *Chemistry and Industry*, 6, 193 (1987)

(20) Javed, K.H. and Thornton, J.D., *Institution of the Chemical Engineers Symposium Series No.88*, 203 (1984).

(21) Thornton, J.D., Anderson, T.J., Javed, K.H. and Achwal, S.K., *Journal of the American Institution of Chemical Engineers*, 31, 7, 1069 (1985).

(22) Batey, W. and Thornton, J.D., *Industrial and Engineering Chemistry Research*, 28, 1101 (1989).

(23) Javed, K.H., Thornton, J.D. and Anderson, T.J., *Journal of the American Institution of Chemical Engineers*, 35, 7, 1125 (1989).

(24) Sherwood, T.K. and Wei, J.C., *Industrial and Engineering Chemistry*, 49, 1030 (1957).

(25) Thompson, P.J., Batey, W. and Watson, R.J., *Institution of Chemical Engineers Symposium Series*, 88, 231 (1984).

(26) Lewis, J.B. and Pratt, H.R.C., *Nature*, London, 171, 1155 (1953).

(27) Batey, W., Lonie, S.J., Thompson, P.J. and Thornton, J.D., *Institution of the Chemical Engineers Symposium Series No.*38, 57 (1984).

(28) Thompson, P.J. and Perez de Ortiz, E.S., *ACTES, ENSIGC*, Toulouse, D–II–1 (1987)

(29) Pichugin, A.A., Tarasov, V.V, Arutiunyan, V.A. and Goryachev, S.V., *Proceedings International Solvent Extraction Conference*, Moscow (1988).

(30) Nakache, E., Dupeyrat, M. and Lemaire, J., *Journal de Chimie Physique et de Physico–Chemie Biologique*, 83, 339 (1986).

(31) Nakache, E. and Dupeyrat, M. , *Journal de Chimie Physique*, 79, 563 (1982).

(32) Nakache, E. and Dupeyrat, M., *Faraday Discussions of the Chemical Society*, 77, 13, (1984).

(33) Nakache, E., Dupeyrat, M. and Vignes–Adler, M., *Journal of Colloid and Interface Science*, 94,187 (1983).

(34) Sanfeld, A. and Steinchen, A., *Faraday Discussions of the Chemical Society*, 77, 11 (1984).

(35) Sanfeld, A. and Steinchen, A., *Biophysical Chemistry*, 3, 99, (1975).

(36) Deyhimi, F. and Sanfeld, A., *C.R. Academy of Science Paris*, 279, 437 (1974).

(37) Sanfeld, A. and Steinchen, A., *Chemical Physics*, 1, 156 (1973).

(38) Hennenberg, M., Sorensen, T.S., Steinchen, A. and Sanfeld, A., *Journal de Chimie Physique*, 72, 1202 (1975).

(39) Sorensen, T.S., *Journal of the Chemical Society, Faraday Transactions Section II*, 76, 1170 (1980)

(40) Ruckenstein, E. and Berbente, C., *Chemical Engineering Science*, 19, 329 (1964).

(41) Benard, H., *Annales de Chimie et de Physique*, 23, 62 (1901).

(42) Rayleigh, Lord, *Phylosophical Magazine*, 32, 529, (1916).

(43) Austin, L.J. and Sawistowski, H., *Institution of the Chemical Engineers Symposium Series No.26* (1967).

(44) Mel, H.C., *Chemical Engineering Science*, 19, 847 (1964)

(45) Ostrach, S., *Transactions of the American Society of Mechanical Engineering*, 79, 299 (1957).

(46) Austin, L.J., *PhD Thesis*, University of London (1966).

(47) Berg, J.C. and Morig, C.R., *Chemical Engineering Science*, 24, 937 (1969).

(48) Bruckner, R., *European Space Agency, Proceedings of the European Symposium*, ESA SP–142, 267 (1979).

(49) Bruckner, R., *Space Research*, 19, 511 (1979).

(50) Walter, H.U., *European Space Agency, Proceedings of the European Symposium*, ESA SP–219, 47 (1984).

(51) Fredriksson, H., *European Space Agency, Proceedings of the European Symposium*, ESA SP–256, 151 (1987).

(52) Schwabe, D. and Scharmann, A., *Advance Space Research*, vol 3, 5, 89 (1983).

(53) Schwabe, D. and Scharmann, A., *Advance Space Research*, vol 4, 5, 43 (1984).

(54) Schwabe, D. and Scharmann, A., *Proceedings of the 5th Symposium on Material Sciences under Microgravity*, ESA SP–222 (1984).

(55) Siekmann, J., Wozniak, G., Srulijes, J., Nahle, R., Neuhaus, D.,*European Space Agency, Proceedings of the European Symposium*, ESA SP–256, 179 (1987).

(56) Legros, J.C., Limbourg–Fontaine, Petre, G., *Acta Astronautica*, vol 11, 2, 143 (1984).

(57) Legros, J.C., Limbourg–Fontaine, Petre, G., *European Space Agency, Proceedings of the European Symposium*, ESA SP–256, 245 (1987).

(58) Villers, D. and Platten, J.K., *Proceedings of the 5th Symposium on Material Sciences under Microgravity*, ESA SP–222 (1984).

(59) Villers, D. and Platten, J.K., *Physico Chemical Hydrodynamics*, 8, 173 (1987)

(60) Lebon, G. and Cloot, A., *Acta Mechanica*, 43, 141 (1982).

(61) Napolitano, L.G., Golia, C. and Viviani, A., *Proceedings of the 5th Symposium on Material Sciences under Microgravity*, ESA SP–222 (1984).

(62) Napolitano, L.G., Monti, R. and Russo, G., *Proceedings of the 5th Symposium on Material Sciences under Microgravity*, ESA SP–222 (1984).

(63) Lam, T.T. and Bayazitoglu, P.L., *Acta Astronautica*, vol 17, 1, 31 (1988).

(64) Oliver, D.L.R. and Dewitt, K.J., *International Journal of Heat and Mass Transfer*, vol 31, 7,1534 (1988).

(65) Maekawa, T. and Tanasawa, I., *European Space Agency, Proceedings of the European Symposium*, ESA SP–256, 493 (1987).

(66) Turner, J.S., *Buoyancy effects in fluids*, Cambridge University Press, Cambridge (1973).

(67) Lee, J. Hycen, M.T. and Kim, K.W., *International Journal of Heat and Mass Transfer*, 31, 1969 (1988).

(68) Sawistowski, H., *Ber. Bunsenges. Phys. Chem.* 85, 905 (1981).

(69) Rogers, D., Thompson, P.J. and Thornton, J.D., *Institution of Chemical Engineers Symposium Series No.103*, 15 (1987).

(70) Boussinesq, J., *Ann. Chim. Phys.* 29, 349 (1913).

(71) Ajawin, L.A., *PhD Thesis*, University of London (1980).

(72) Murthy, C.V.R., *PhD Thesis*, University of London (1987).